Light-Matter Interaction Hamiltonians in Cavity Quantum Electrodynamics

Michael A.D. Taylor,[1, a)] Arkajit Mandal,[2, b)] and Pengfei Huo[3, 1, c)]
[1)] *Institute of Optics, Hajim School of Engineering, University of Rochester, Rochester, New York, 14627, U. S. A.*
[2)] *Department of Chemistry, Texas A &M University, College Station, TX 77842, U. S. A.*
[3)] *Department of Chemistry, University of Rochester, 120 Trustee Road, Rochester, New York 14627, U. S. A.*

CONTENTS

[a)] Electronic mail: michael.taylor@rochester.edu
[b)] Electronic mail: mandal@tamu.edu
[c)] Electronic mail: pengfei.huo@rochester.edu

I. INTRODUCTION

Recent progress in enabling new chemical reactivities by strongly coupling molecular systems to quantized radiation[1–12] has stimulated theoretical developments in molecular quantum electrodynamics[13–29]. In particular, light-matter interactions beyond the weak-strong coupling regime, such as the ultra-strong coupling[28] (USC) and the deep-strong coupling[30] (DSC) regime, are currently an active field of theoretical research[13,18,20,30–37]. Such coupling regimes lead to new exciting physical phenomena that cannot be described with the widely used approximate light-matter Hamiltonians such as the Rabi and Jaynes-Cumming Hamiltonians[18,19,21,24,38] of quantum optics. In this manner, it is crucial to strategically choose which light-matter Hamiltonian to use to model your system by understanding the different benefits and shortcomings of each representation.

As this field of cavity quantum electrodynamics (cQED) is highly interdisciplinary drawing from both quantum optics and physical chemistry, the appropriate choice of Hamiltonian can be obfuscated for those new to the field. Often, the relationships between Hamiltonians and exact levels of approximation consequentially become unclear. In this review, we seek to put in one place all the major gauges and representations commonly used in the field in one place with detailed derivations that relate them to each other, helping to bridge the gap between quantum optics and physical chemistry.

This review is organized such that exact Hamiltonians for matter coupled to a single mode are initially introduced, and the following three sections layer on approximations, going all the way to the semiclassical approximation. As such, Sect. II introduces different forms of the full Hilbert space Hamiltonian, derived from the fundamental Minimal Coupling Hamiltonian. Then, in Sect. III, the truncation of the full Hilbert space is considered, with discussions of the various methods for addressing the gauge ambiguities caused by such projections. In Sect. IV, the simplified quantum optics models are discussed and benchmarked relative to the truncated matter Hamiltonians. Then, Sect. V provides a brief comparison of cQED methods with Floquet theory, which is under the semiclassical approximation. Using insights from this path, Sect. VI extends the formalism to more generalized forms of cQED Hamiltonians for systems with many modes and many molecules. The future perspectives and analysis are provided in Sect. VII.

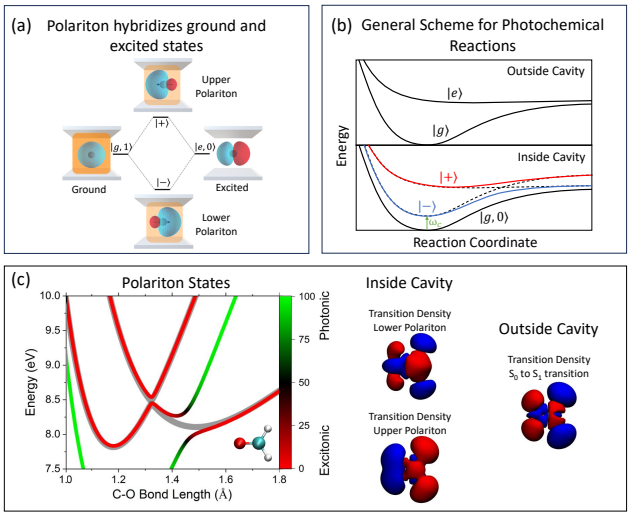

FIG. 1. Characteristic examples of polariton photochemistry. (a) Schematic illustration of Rabi splitting due to strong coupling for a single atom in a cavity. (b) Eigenspectra for a diatomic molecular system both outside and inside a cavity. (c) Properties of a formaldehyde molecule inside a cavity, demonstrating more complex polariton eigenspectra and changes in transition densities due to the cavity.[39]

II. CAVITY QED HAMILTONIANS

Before directly discussing various exact cavity QED Hamiltonians, we define the formalism used in the rest of the review for the two primary degrees of freedom (DOF) covered in this review, namely the molecular Hamiltonian and the photonic Hamiltonian. Following this brief overview of these independent Hamiltonians, the rest of this section focuses on different representations of QED Hamiltonians that describe light-matter interactions: the minimal coupling Hamiltonian (Sect. II A), the dipole gauge Hamiltonian (Sect. II B), and the assymptotically decoupled Hamiltonian (Sect. II C).

We begin by defining the matter Hamiltonian and the corresponding total dipole operator as follows

$$\hat{H}_{\mathrm{M}} = \hat{\mathbf{T}} + \hat{V}(\hat{\mathbf{x}}) = \sum_j \frac{1}{2m_j}\hat{\mathbf{p}}_j^2 + \hat{V}(\hat{\mathbf{x}});\ \hat{\boldsymbol{\mu}} = \sum_j z_j \hat{\mathbf{x}}_j, \quad (1)$$

where j is the index of the j_{th} charged particle (including all electrons and nuclei), with the corresponding mass m_j and charge z_j. In addition, $\hat{\mathbf{x}} \equiv \{\hat{\mathbf{x}}_j\} = \{\hat{\mathbf{R}}, \hat{\mathbf{r}}\}$ with $\hat{\mathbf{R}}$ and $\hat{\mathbf{r}}$ representing the sets of nuclear and electronic coordinates, respectively, $\hat{\mathbf{p}} \equiv \{\hat{\mathbf{p}}_{\mathbf{R}}, \hat{\mathbf{p}}_{\mathbf{r}}\} \equiv \{\hat{\mathbf{p}}_j\}$ is the *mechanical* momentum operator as well as the canonical momentum operator, such that $\hat{\mathbf{p}}_j = -i\hbar\boldsymbol{\nabla}_j$. Further, $\hat{\mathbf{T}} = \hat{\mathbf{T}}_{\mathbf{R}} + \hat{\mathbf{T}}_{\mathbf{r}}$ is the kinetic energy operator, where $\hat{\mathbf{T}}_{\mathbf{R}}$ and $\hat{\mathbf{T}}_{\mathbf{r}}$ represent the kinetic energy operator for nuclei and for electrons, respectively, and $\hat{V}(\hat{\mathbf{x}})$ is the potential operator that describes the Coulombic interactions among electrons and nuclei. For a more in-depth review of molecular Hamiltonians, see Appendix A.

The cavity photon field Hamiltonian under the single mode assumption is expressed as

$$\hat{H}_{\mathrm{ph}} = \hbar\omega_{\mathrm{c}}\big(\hat{a}^\dagger\hat{a} + \frac{1}{2}\big) = \frac{1}{2}\big(\hat{p}_{\mathrm{c}}^2 + \omega_{\mathrm{c}}^2\hat{q}_{\mathrm{c}}^2\big), \quad (2)$$

where ω_{c} is the frequency of the mode in the cavity, $\hat{a}^\dagger$ and $\hat{a}$ are the photonic creation and annihilation operators, and $\hat{q}_{\mathrm{c}} = \sqrt{\hbar/2\omega_{\mathrm{c}}}(\hat{a}^\dagger + \hat{a})$ and $\hat{p}_{\mathrm{c}} = i\sqrt{\hbar\omega_{\mathrm{c}}/2}(\hat{a}^\dagger - \hat{a})$ are the photonic coordinate and momentum operators, respectively. Choosing the Coulomb gauge, $\boldsymbol{\nabla}\cdot\hat{\mathbf{A}} = 0$, the vector potential becomes purely transverse $\hat{\mathbf{A}} = \hat{\mathbf{A}}_\perp$. Under the long-wavelength approximation,

$$\hat{\mathbf{A}} = \mathbf{A}_0\big(\hat{a} + \hat{a}^\dagger\big) = \mathbf{A}_0\sqrt{2\omega_{\mathrm{c}}/\hbar}\ \hat{q}_{\mathrm{c}}, \quad (3)$$

where $\mathbf{A}_0 = \sqrt{\frac{\hbar}{2\omega_{\mathrm{c}}\varepsilon_0\mathcal{V}}}\ \hat{\mathbf{e}}$ for a Fabry–Pérot cavity, with $\mathcal{V}$ as the quantization volume inside the cavity, ε_0 as the permittivity, and $\hat{\mathbf{e}}$ is the unit vector of the field polarization. For a more in-depth review of quantum optics and QED, see Appendix B.

A. The Minimal Coupling Hamiltonian

The minimal coupling QED Hamiltonian in the *Coulomb* gauge (the "p · A" form) is expressed as

$$\hat{H}_{\mathrm{p\cdot A}} = \sum_j \frac{1}{2m_j}(\hat{\mathbf{p}}_j - z_j\hat{\mathbf{A}})^2 + \hat{V}(\hat{\mathbf{x}}) + \hat{H}_{\mathrm{ph}}, \quad (4)$$

where $\hat{\mathbf{p}}_j = -i\hbar\boldsymbol{\nabla}_j$ is the *canonical* momentum operator for the j_{th} particle.

We further introduce the Power-Zienau-Woolley (PZW) gauge transformation operator[40,41] as

$$\hat{U} = \exp\big[-\frac{i}{\hbar}\hat{\boldsymbol{\mu}}\cdot\hat{\mathbf{A}}\big] = \exp\big[-\frac{i}{\hbar}\hat{\boldsymbol{\mu}}\cdot\mathbf{A}_0\big(\hat{a} + \hat{a}^\dagger\big)\big], \quad (5)$$

or $\hat{U} = \exp\big[-\frac{i}{\hbar}\sqrt{2\omega_{\mathrm{c}}/\hbar}\hat{\boldsymbol{\mu}}\mathbf{A}_0\hat{q}_{\mathrm{c}}\big] = \exp\big[-\frac{i}{\hbar}(\sum_j z_j\hat{\mathbf{A}}\hat{\mathbf{x}}_j)\big]$. Recall that a momentum boost operator $\hat{U}_{\mathrm{p}} = e^{-\frac{i}{\hbar}p_0\hat{q}}$ displaces $\hat{p}$ by the amount of p_0, such that $\hat{U}_{\mathrm{p}}\hat{O}(\hat{p})\hat{U}_{\mathrm{p}}^\dagger = \hat{O}(\hat{p} + p_0)$. Hence, $\hat{U}$ is a boost operator for both the photonic momentum $\hat{p}_{\mathrm{c}}$ by the amount of $\sqrt{2\omega_{\mathrm{c}}/\hbar}\hat{\boldsymbol{\mu}}\mathbf{A_0}$, as well as for the matter momentum $\hat{\mathbf{p}}_j$ by the amount of $z_j\hat{\mathbf{A}}$. The PZW gauge operator (Eqn. 5) is a special case of $\hat{U}_\chi$, such that $\chi = -\hat{\mathbf{x}}_j\cdot\hat{\mathbf{A}}$. Using $\hat{U}^\dagger$ to boost the matter momentum, one can show that

$$\hat{H}_{\mathrm{p\cdot A}} = \hat{U}^\dagger\hat{H}_{\mathrm{M}}\hat{U} + \hat{H}_{\mathrm{ph}}, \quad (6)$$

hence $\hat{H}_{\mathrm{p\cdot A}}$ can be obtained[31] by a momentum boost with the amount of $-z_j\hat{\mathbf{A}}$ for $\hat{\mathbf{p}}_j$, then adding $\hat{H}_{\mathrm{ph}}$.

B. The Dipole Gauge Hamiltonian

The QED Hamiltonian under the *dipole* gauge (the "d · E" form[40,42]) can be obtained by performing the

PZW transformation on $\hat{H}_{\text{p·A}}$ as follows

$$\hat{H}_{\text{d·E}} = \hat{U}\hat{H}_{\text{p·A}}\hat{U}^\dagger = \hat{U}\hat{U}^\dagger\hat{H}_{\text{M}}\hat{U}\hat{U}^\dagger + \hat{U}\hat{H}_{\text{ph}}\hat{U}^\dagger \tag{7}$$
$$= \hat{H}_{\text{M}} + \hbar\omega_{\text{c}}(\hat{a}^\dagger\hat{a} + \frac{1}{2}) + i\omega_{\text{c}}\hat{\boldsymbol{\mu}}\cdot\mathbf{A}_0(\hat{a}^\dagger - \hat{a}) + \frac{\omega_{\text{c}}}{\hbar}(\hat{\boldsymbol{\mu}}\cdot\mathbf{A}_0)^2,$$

where we have used Eqn. 6 to express $\hat{H}_{\text{p·A}}$, and the last three terms of the above equation are the results of $\hat{U}\hat{H}_{\text{ph}}\hat{U}^\dagger$. Using $\hat{q}_{\text{c}}$ and $\hat{p}_{\text{c}}$, one can instead show that

$$\hat{H}_{\text{d·E}} = \hat{H}_{\text{M}} + \frac{1}{2}\omega_{\text{c}}^2\hat{q}_{\text{c}}^2 + \frac{1}{2}(\hat{p}_{\text{c}} + \sqrt{\frac{2\omega_{\text{c}}}{\hbar}}\hat{\boldsymbol{\mu}}\mathbf{A}_0)^2, \tag{8}$$

because the PZW operator boosts the photonic momentum $\hat{p}_{\text{c}}$ by $\sqrt{2\omega_{\text{c}}/\hbar}\hat{\boldsymbol{\mu}}\mathbf{A}_0$. The term $\frac{\omega_{\text{c}}}{\hbar}(\hat{\boldsymbol{\mu}}\mathbf{A}_0)^2$ is commonly referred to as the dipole self-energy (DSE).

The widely used Pauli-Fierz (PF) QED Hamiltonian[17,21,39,43–50] in recent studies of polariton chemistry can be obtained by using the following unitary transformation

$$\hat{U}_\phi = \exp\Big[-i\frac{\pi}{2}\hat{a}^\dagger\hat{a}\Big]. \tag{9}$$

Note that $\hat{U}_\phi\hat{a}^\dagger\hat{a}\hat{U}_\phi^\dagger = \hat{a}^\dagger\hat{a}$, $\hat{U}_\phi\hat{a}\hat{U}_\phi^\dagger = i\hat{a}$, and $\hat{U}_\phi\hat{a}^\dagger\hat{U}_\phi^\dagger = -i\hat{a}^\dagger$, applying $\hat{U}_\phi$ on $\hat{H}_{\text{d·E}}$, we have the PF Hamiltonian as follows

$$\hat{H}_{\text{PF}} = \hat{U}_\phi\hat{H}_{\text{d·E}}\hat{U}_\phi^\dagger \tag{10}$$
$$= \hat{H}_{\text{M}} + \hbar\omega_{\text{c}}(\hat{a}^\dagger\hat{a} + \frac{1}{2}) + \omega_{\text{c}}\hat{\boldsymbol{\mu}}\cdot\mathbf{A}_0(\hat{a} + \hat{a}^\dagger) + \frac{\omega_{\text{c}}}{\hbar}(\hat{\boldsymbol{\mu}}\cdot\mathbf{A_0})^2$$
$$= \hat{H}_{\text{M}} + \frac{1}{2}\hat{p}_{\text{c}}^2 + \frac{1}{2}\omega_{\text{c}}^2\big(\hat{q}_{\text{c}} + \sqrt{\frac{2}{\hbar\omega_{\text{c}}}}\hat{\boldsymbol{\mu}}\cdot\mathbf{A_0}\big)^2$$

The above PF Hamiltonian has the advantage as a pure real Hamiltonian and the photonic DOF can be viewed[21,43] and computationally treated[51,52] as an additional "nuclear coordinate".

We emphasize that both the **operators** as well as the **wavefunctions** should be Gauge transformed (though $\hat{U}$), in order to have a Gauge invariant expectation values. This means that

$$\hat{O} \to \hat{U}\hat{O}\hat{U}^\dagger, \qquad |\Psi\rangle \to \hat{U}|\Psi\rangle, \tag{11}$$

such that $\langle\hat{O}\rangle = \langle\Psi|\hat{O}|\Psi\rangle = (\langle\Psi|\hat{U}^\dagger)(\hat{U}\hat{O}\hat{U}^\dagger)(\hat{U}|\Psi\rangle)$.

This argument also applies to the photon number operator, which means that it should also be gauge transformed in order to provide a physical result.[18,20] Under the Coulomb gauge, it is defined as

$$\hat{N}_{\text{p·A}} = \hat{a}^\dagger\hat{a} = \frac{1}{2\hbar\omega_{\text{c}}}\hat{p}_{\text{c}}^2 + \frac{\omega_{\text{c}}}{2\hbar}\hat{q}_{\text{c}}^2 - \frac{1}{2} \tag{12}$$

Under the dipole gauge, it should be

$$\hat{N}_{\text{d·E}} = \hat{U}\hat{a}^\dagger\hat{a}\hat{U}^\dagger = \hat{U}\hat{a}^\dagger\hat{U}^\dagger\hat{U}\hat{a}\hat{U}^\dagger \equiv \hat{d}^\dagger\hat{d}, \tag{13}$$
$$= \frac{1}{2\hbar\omega_{\text{c}}}(\hat{p}_{\text{c}} + \sqrt{\frac{2\omega_{\text{c}}}{\hbar}}\hat{\boldsymbol{\mu}}\mathbf{A}_0)^2 + \frac{\omega_{\text{c}}}{2\hbar}\hat{q}_{\text{p·A}}^2 - \frac{1}{2}$$

where $\hat{d}^\dagger = \hat{U}\hat{a}^\dagger\hat{U}^\dagger = \sqrt{\frac{\omega_{\text{c}}}{2\hbar}}\hat{U}(\hat{q}_{\text{c}} - \frac{i}{\omega}\hat{p}_{\text{c}})\hat{U}^\dagger = \sqrt{\frac{\omega_{\text{c}}}{2\hbar}}[\hat{q}_{\text{c}} - \frac{i}{\omega}(\hat{p}_{\text{c}} + \sqrt{2\omega_{\text{c}}/\hbar}\hat{\boldsymbol{\mu}}\mathbf{A}_0)]$. For the PF Hamiltonian, the photon number operator should be

$$\hat{N}_{\text{PF}} = \hat{U}_\phi\hat{U}\hat{a}^\dagger\hat{a}\hat{U}^\dagger\hat{U}_\phi^\dagger = (\hat{U}_\phi\hat{U}\hat{a}^\dagger\hat{U}^\dagger\hat{U}_\phi^\dagger)(\hat{U}_\phi\hat{U}\hat{a}\hat{U}^\dagger\hat{U}_\phi^\dagger) \equiv \hat{c}^\dagger\hat{c}$$
$$= \frac{1}{2\hbar\omega_{\text{c}}}\hat{p}_{\text{c}}^2 + \frac{\omega_{\text{c}}}{2\hbar}(\hat{q}_{\text{c}} + \sqrt{\frac{2}{\hbar\omega_{\text{c}}}}\hat{\boldsymbol{\mu}}\cdot\mathbf{A_0})^2 - \frac{1}{2}, \tag{14}$$

where

$$\hat{c}^\dagger = \hat{U}_\phi\hat{U}\hat{a}^\dagger\hat{U}^\dagger\hat{U}_\phi^\dagger = \sqrt{\frac{\omega_{\text{c}}}{2\hbar}}\big[(\hat{q}_{\text{c}} + \sqrt{\frac{2\omega_{\text{c}}}{\hbar}}\hat{\boldsymbol{\mu}}\mathbf{A}_0)) - \frac{i}{\omega_{\text{c}}}\hat{p}_{\text{c}}\big], \tag{15}$$

and the physical number operator is then

$$\hat{N} = \hat{U}_\phi\hat{U}\hat{a}^\dagger\hat{a}\hat{U}^\dagger\hat{U}_\phi^\dagger = \hat{c}^\dagger\hat{c} \neq \hat{a}^\dagger\hat{a}. \tag{16}$$

This has been pointed out extensively in the previous reference, and recently in Ref. 18,20. Using the incorrect expression $\hat{a}^\dagger\hat{a}$ under the dipole gauge will overestimate the actual photon number, causing inaccurate and misleading results.

C. Asymptotically Decoupled Hamiltonian

While the Coulomb and dipole gauges are by far the most common representations for light-matter couplings, in recent works, the Asymptotically Decoupled Hamiltonian was introduced to increase the simulation accuracy for models with arbitrarily strong coupling strengths[35,53]. We begin by rewriting $\hat{H}_{\text{p·A}}$ from Eq. 4 in its expanded form,

$$\hat{H}_{\text{p·A}} = \hat{H}_{\text{M}} + \hbar\omega_c\hat{a}^\dagger\hat{a} + \frac{\hat{\mathbf{p}}\cdot\mathbf{A_0}}{m}(\hat{a}^\dagger + \hat{a}) + \frac{|\mathbf{A_0}|^2}{2m}(\hat{a}^\dagger + \hat{a})^2, \tag{17}$$

where the zero point energy of the photonic mode is omitted for simplicity. Then we perform a Bogoliubov transformation on the photonic degrees of freedom to rewrite $\hat{H}_{\text{p·A}}$ as,

$$\hat{H}_{\text{p·A}} = \hat{H}_{\text{M}} + \hbar\Omega\hat{b}^\dagger\hat{b} - x_\Omega\mathbf{g}\cdot\hat{\mathbf{p}}(\hat{b}^\dagger + \hat{b}), \tag{18}$$

where $\Omega = \sqrt{\omega_c^2 + 2N|\mathbf{g}|^2}$ is the dressed photon frequency with a particle number N, $\mathbf{g} = q\mathbf{A_0}\sqrt{\omega_c/m\hbar}$ is the coupling strength, and $x_\Omega = \sqrt{\hbar/m\Omega}$ is a characteristic length. The Bogoliubov transform used in Eqn. 18 is of the form, $\hat{b} + \hat{b}^\dagger = \sqrt{\Omega/\omega_c}(\hat{a} + \hat{a}^\dagger)$ to remove the linear term in $(\hat{a} + \hat{a}^\dagger)$ from Eqn. 17.

Recall that a position shift operator, $\hat{U}_q = e^{-\frac{i}{\hbar}q_0\hat{p}}$ displaces $\hat{q}$ by the amount q_0, such that $\hat{U}_q\hat{O}(\hat{q})\hat{U}_q^\dagger = \hat{O}(\hat{q} + q_0)$. With this in mind, a shift operator in both photonic and matter coordinates is introduced, which transforms Eq. 18 into the AD representation.

$$\hat{U}_{\text{AD}} = \exp\left\{\left[-\frac{i}{\hbar}\xi_{\mathbf{g}}\cdot\hat{\mathbf{p}}\hat{\pi}\right]\right\} \tag{19}$$

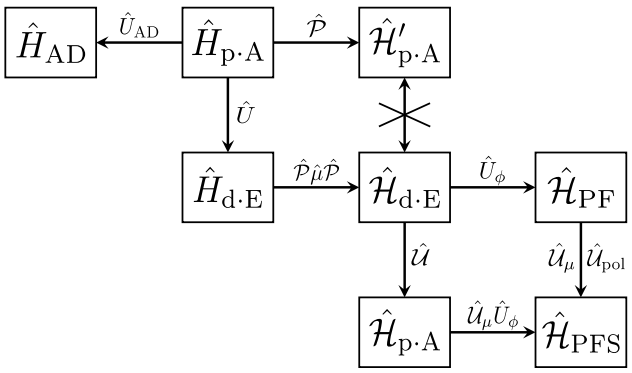

FIG. 2. Block diagram describing the relationships between various Hamiltonians discussed in this article. Hamiltonians in the top row have poor matter state convergence properties. Hamiltonians in the second row have poor Fock state convergence properties. Hamiltonians in the bottom row have good matter and Fock state convergence properties.

where $\hat{\pi} = i(\hat{b}^\dagger - \hat{b})$ is the photonic momentum in the Bogoliubov transformed space and $\xi_{\mathbf{g}} = \mathbf{g}x_\Omega/\Omega$ is an effective coupling parameter in the AD representation. This leads to the introduction of the AD Hamiltonian, $\hat{H}_{\mathrm{AD}} = \hat{U}^\dagger_{\mathrm{AD}}\hat{H}_{\mathrm{p\cdot A}}\hat{U}_{\mathrm{AD}}$,

$$\hat{H}_{\mathrm{AD}} = \sum_j \frac{1}{2m_j}\hat{\mathbf{p}}_j^2 + \hat{V}(\hat{\mathbf{x}}_j + \xi_{\mathbf{g}}\hat{\pi}) + \hbar\Omega\hat{b}^\dagger\hat{b} - \sum_j \frac{\hbar^2 g^2}{m_j\Omega^2}\hat{\mathbf{p}}_j^2 \tag{20}$$

By rescaling the mass of each particle to an effective mass, $m_j^{\mathrm{eff}} = m_j[1 + 2|\mathbf{g}/\omega_c|^2]$, this Asymptotically Decoupled Hamiltonian is then simplified to,

$$\hat{H}_{\mathrm{AD}} = \sum_j \frac{1}{2m_j^{\mathrm{eff}}}\hat{\mathbf{p}}_j^2 + \hat{V}(\hat{\mathbf{x}}_j + \xi_{\mathbf{g}}\hat{\pi}) + \hbar\Omega\hat{b}^\dagger\hat{b} \tag{21}$$

This is simply a photonic Hamiltonian added to a matter Hamiltonian with an effective mass scaling in the kinetic energy and a shift in coordinates in the potential energy. Note that the coupling is mediated by the shifting of each $\mathbf{x_j}$ by the photonic operator weighted by an effective coupling term $\xi_{\mathbf{g}}$. However, $|\xi_{\mathbf{g}}(\mathbf{g})|$ has a finite peak and then asymptotically approaches zero for large $|\mathbf{g}|$. In other words, in this representation the photonic and matter degrees of freedom asymptotically decouple at arbitrarily high coupling strength. For this reason, this representation was put forward as a convenient Hamiltonian when considering systems in the deep strong coupling regime and beyond.

This AD Hamiltonian has also been expanded upon in recent work for solid-state materials in reciprocal space in Ref. 53, but is beyond the scope of this review as we are focused on molecular QED.

III. QED HAMILTONIANS IN TRUNCATED HILBERT SPACES

Investigating the cavity QED computationally always requires a truncation of electronic states applied to the QED Hamiltonians[31,33], as the electronic Hilbert space in principle has an infinite basis size for any real system. Additionally, as these matter electronic states are often difficult to obtain, one typically projects the QED Hamiltonian to a few physically relevant electronic states, which can still produce accurate results in the low energy regime. However, when dealing with strong light-matter coupling, the manner in which the truncation of the Hilbert space is performed drastically changes the accuracy and consequentially the convergence of results with basis size. As such, this section reviews the recent literature results on truncating the Hilbert space of these QED systems. Sects. III A and III B discuss two different ways to truncate the matter DOF of the dipole and Coulomb gauge Hamiltonians from Sects. II A and II B. Then, Sect. III C discusses a new representation of the light-matter coupling in a truncated Hilbert space, the polarized Fock state (PFS) Hamiltonian. Finally, Sects. III D and III E briefly discuss how performing truncations applies for more general systems with many modes and beyond the long-wavelength approximation, respectively (Note that the full descriptions for these generalized systems are found in Sect. VI).

To accurately illustrate the performance of different truncated QED Hamiltonians, we test the accuracy of the Hamiltonians discussed in this review on a model molecular system inside a cavity. Fig. 3 shows the potential energy surfaces, diabatic potentials and dipole matrix elements of the model system that we use to benchmark these Hamiltonians, the so-called Shin-Metiu proton-transfer model system. This Shin-Metiu model molecular system[54] contains two fixed ions, one moving electron and a proton (whose position is R), all interacting with each other through modified Coulombic potentials.

A. Dipole and Coulomb Gauge Hamiltonians

We begin with the simplest case of matter truncation. Consider a finite subset of electronic states $\{|\alpha\rangle\}$, where the projection operator $\hat{\mathcal{P}} = \sum_\alpha |\alpha\rangle\langle\alpha|$ defines the truncation of the full electronic Hilbert space $\hat{\mathbb{1}}_{\mathrm{r}} = \hat{\mathcal{P}} + \hat{\mathcal{Q}}$ to the corresponding subspace $\hat{\mathcal{P}}$. This truncation reduces the size of the Hilbert space from originally $\hat{\mathbb{1}}_{\mathrm{r}} \otimes \hat{\mathbb{1}}_{\mathrm{R}} \otimes \hat{\mathbb{1}}_{\mathrm{ph}}$ to now $\hat{\mathcal{P}} \otimes \hat{\mathbb{1}}_{\mathrm{R}} \otimes \hat{\mathbb{1}}_{\mathrm{ph}}$, where $\hat{\mathbb{1}}_{\mathrm{R}}$ and $\hat{\mathbb{1}}_{\mathrm{ph}}$ represent the identity operators of the nuclear and photonic DOF, respectively. The truncated matter Hamiltonian is

$$\hat{\mathcal{H}}_{\mathrm{M}} = \hat{\mathcal{P}}\hat{H}_{\mathrm{M}}\hat{\mathcal{P}} = \hat{\mathcal{P}}\hat{\mathbf{T}}\hat{\mathcal{P}} + \hat{\mathcal{P}}\hat{V}(\hat{\mathbf{x}})\hat{\mathcal{P}}. \tag{22}$$

Throughout this review, we use calligraphic symbols (such as $\hat{\mathcal{H}}_{\mathrm{M}}$) to indicate operators in the truncated Hilbert space.

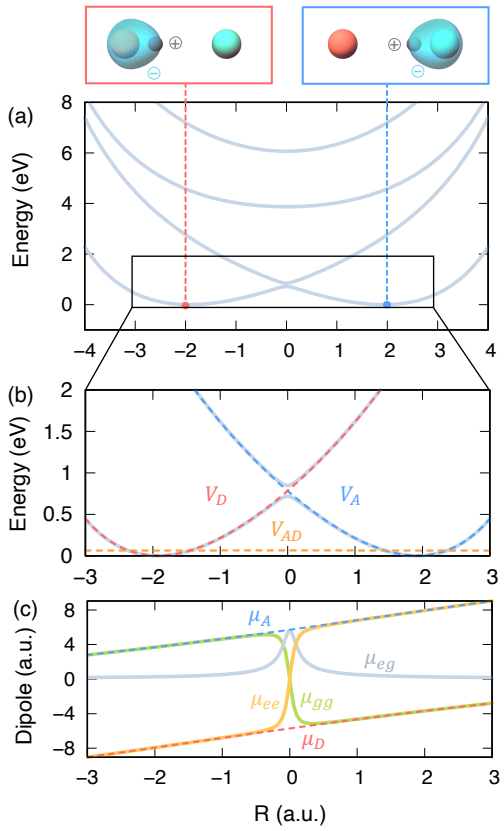

FIG. 3. Shin-Metiu model molecular system. (a) Potential energy surfaces of the first four molecular states. (b) Diabatic potentials (dashed curves) $V_{\mathrm{d\cdot E}}(R)$ (red) and $V_{\mathrm{A}}(R)$ (blue), with diabatic coupling V_{AD} (gold). (c) Matrix elements of $\hat{\mu}$ in the adiabatic representation (solid) μ_{gg} (green), μ_{ee} (orange), and μ_{eg} (light blue), as well as in the diabatic representation (dashed curves) $\mu_{\mathrm{d\cdot E}}$ (red) and μ_{A} (blue).

The simplest way to then write the QED Hamiltonians from Sects. II A and II B in this truncated subspace would then be to truncate each matter operator by $\hat{\mathcal{P}}$. Truncating the momentum operator and dipole operator as $\hat{\mathcal{P}}\hat{\mathbf{p}}_j\hat{\mathcal{P}}$ and $\hat{\mathcal{P}}\hat{\boldsymbol{\mu}}\hat{\mathcal{P}}$, the QED Hamiltonians under the truncated subspace are commonly defined as

$$\hat{\mathcal{H}}'_{\mathrm{p\cdot A}} = \hat{\mathcal{P}}\hat{U}^\dagger\hat{H}_{\mathrm{M}}\hat{U}\hat{\mathcal{P}} + \hat{H}_{\mathrm{ph}} \tag{23a}$$
$$= \hat{\mathcal{H}}_{\mathrm{M}} + \hat{H}_{\mathrm{ph}} + \sum_j \Big(-\frac{z_j}{m_j}\hat{\mathcal{P}}\hat{\mathbf{p}}_j\hat{\mathcal{P}}\hat{\boldsymbol{A}} + \frac{z_j^2\hat{\boldsymbol{A}}^2}{2m_j}\Big)$$
$$\hat{\mathcal{H}}_{\mathrm{d\cdot E}} = \hat{\mathcal{H}}_{\mathrm{M}} + \hat{H}_{\mathrm{ph}} + i\omega_{\mathrm{c}}\hat{\mathcal{P}}\hat{\boldsymbol{\mu}}\hat{\mathcal{P}}\mathbf{A}_0(\hat{a}^\dagger - \hat{a}) \tag{23b}$$
$$+ \frac{\omega_{\mathrm{c}}}{\hbar}(\hat{\mathcal{P}}\hat{\boldsymbol{\mu}}\hat{\mathcal{P}}\mathbf{A}_0)^2.$$

Note that $\hat{\mathcal{H}}'_{\mathrm{p\cdot A}} = \hat{\mathcal{P}}\hat{H}_{\mathrm{p\cdot A}}\hat{\mathcal{P}} = \hat{\mathcal{P}}\hat{U}^\dagger\hat{H}_{\mathrm{M}}\hat{U}\hat{\mathcal{P}} + \hat{H}_{\mathrm{ph}}$. It is well known that the above two Hamiltonians do not generate the same polariton eigenspectrum[31,33,37,55–59] under the ultra-strong coupling regime[28], explicitly breaking down the gauge invariance. This leads to the gauge ambiguity[33,60,61] as to which Hamiltonian, $\hat{\mathcal{H}}'_{\mathrm{p\cdot A}}$ or $\hat{\mathcal{H}}_{\mathrm{d\cdot E}}$, is viable to compute physical quantities when applying $\hat{\mathcal{P}}$. This is attributed[33,52] to the fact that $\hat{\mathcal{H}}'_{\mathrm{p\cdot A}}$ usually requires a larger subset of the matter states to converge or generate consistent results with $\hat{\mathcal{H}}_{\mathrm{d\cdot E}}$, and apparently, under the *complete* basis limit, they are gauge invariant (see Figs. 4(a)-(d)). Further, this fundamentally different behavior of $\hat{\mathcal{H}}'_{\mathrm{p\cdot A}}$ and $\hat{\mathcal{H}}_{\mathrm{d\cdot E}}$ upon state truncation is also attributed to the fundamental asymmetry of the operators $\hat{\mathbf{p}}$ and $\hat{\boldsymbol{\mu}} = \sum_j z_j\hat{\mathbf{x}}_j$[33]. Fig. 4(a)-(d) shows these convergence properties of both the dipole and Coulomb gauge Hamiltonians, demonstrating that for this Shin-Metiu model system, $\hat{\mathcal{H}}'_{\mathrm{p\cdot A}}$ requires 9x more matter states to converge (see panels (c) and (d)).

Performing the same truncation scheme, the PF Hamiltonian in the truncated electronic basis, $\hat{\mathcal{H}}_{\mathrm{PF}} = \hat{U}_\theta\hat{\mathcal{H}}_{\mathrm{d\cdot E}}\hat{U}_\theta^\dagger = \hat{\mathcal{H}}_{\mathrm{M}} + \hat{U}_\theta\hat{\mathcal{U}}\hat{H}_{\mathrm{ph}}\hat{\mathcal{U}}^\dagger\hat{U}_\theta^\dagger$, is expressed as

$$\hat{\mathcal{H}}_{\mathrm{PF}} = \hat{\mathcal{H}}_{\mathrm{M}} + \hat{H}_{\mathrm{ph}} + \omega_{\mathrm{c}}\hat{\mathcal{P}}\hat{\boldsymbol{\mu}}\hat{\mathcal{P}}\cdot\mathbf{A}_0(\hat{a}+\hat{a}^\dagger) + \frac{\omega_{\mathrm{c}}}{\hbar}(\hat{\mathcal{P}}\hat{\boldsymbol{\mu}}\hat{\mathcal{P}}\cdot\mathbf{A_0})^2$$
$$= \hat{\mathcal{H}}_{\mathrm{M}} + \frac{1}{2}\hat{p}_{\mathrm{c}}^2 + \frac{1}{2}\omega_{\mathrm{c}}^2\Big(\hat{q}_{\mathrm{c}} + \sqrt{\frac{2}{\hbar\omega_{\mathrm{c}}}}\hat{\mathcal{P}}\hat{\boldsymbol{\mu}}\hat{\mathcal{P}}\cdot\mathbf{A_0}\Big)^2 \tag{24}$$

Note that $\hat{U}_\theta$ is only a function of the photonic DOF, thus it does not bring any matter operator that was originally confined in $\hat{\mathcal{P}}$ to $\hat{\mathcal{Q}}$. Therefore, $\hat{\mathcal{H}}_{\mathrm{PF}}$ provides consistent results with $\hat{\mathcal{H}}_{\mathrm{d\cdot E}}$, ensuring that there are no ambiguities between $\hat{\mathcal{H}}_{\mathrm{d\cdot E}}$ and $\hat{\mathcal{H}}_{\mathrm{PF}}$.

B. Properly Truncated Coulomb Gauge Hamiltonian

Ref. 36 contends that this gauge ambiguity between the Coulomb and dipole gauges emerges because the $\hat{\mathcal{P}}\hat{U}^\dagger$ and $\hat{U}\hat{\mathcal{P}}$ in $\hat{\mathcal{H}}'_{\mathrm{p\cdot A}}$ (Eq. 23a) do not consistently constrain light-matter interaction operators in the same electronic subspace as those corresponding operators in $\hat{\mathcal{H}}_{\mathrm{d\cdot E}}$. Indeed, all light-matter interaction operators in $\hat{\mathcal{H}}_{\mathrm{d\cdot E}}$ are completely constrained in the subspace $\hat{\mathcal{P}}$. Meanwhile, for $\hat{\mathcal{H}}'_{\mathrm{p\cdot A}}$, the corresponding light-matter interaction operators are not properly contained in $\hat{\mathcal{P}}$, such that some of them enter the subspace $\hat{\mathcal{Q}} = \hat{\mathbb{1}}_{\mathrm{r}} - \hat{\mathcal{P}}$, and as is the case for $\hat{U}\hat{\mathcal{P}} = (\hat{\mathcal{P}} + \hat{\mathcal{Q}})\hat{U}\hat{\mathcal{P}}$. It is also apparent by examining the diamagnetic term $z_j^2\hat{\boldsymbol{A}}^2/2m_j$ in $\hat{\mathcal{H}}'_{\mathrm{p\cdot A}}$ that it is effectively evaluated in the full space[31,33] $\hat{\mathbb{1}}_{\mathrm{r}}$ (based on the Thomas-Reiche-Kuhn sum rule), hence is not properly confined in $\hat{\mathcal{P}}$. This diamagnetic term overestimates what it should be in the subspace[31,33], and by confining it within $\hat{\mathcal{P}}$, the results can be significantly improved[31]. Similarly, using $\hat{\mathcal{P}}\hat{U}\hat{\mathcal{P}}$[31,55] does not resolve this gauge ambiguity either.

Based on the above conjecture, the gauge ambiguity in the truncated electronic subspace will be resolved by defining the following unitary operator

$$\hat{\mathcal{U}} = \exp\Big[-\frac{i}{\hbar}\hat{\mathcal{P}}\hat{\boldsymbol{\mu}}\hat{\mathcal{P}}\cdot\hat{\mathbf{A}}\Big] \equiv \exp\Big[-\frac{i}{\hbar}\tilde{\boldsymbol{\mu}}(\hat{\mathbf{x}},\hat{\mathbf{p}})\cdot\hat{\mathbf{A}}\Big], \tag{25}$$

such that all terms in $\hat{\mathcal{U}} = \sum_{n=0}^{\infty}\frac{1}{n!}(-\frac{i}{\hbar})^n(\hat{\mathcal{P}}\hat{\boldsymbol{\mu}}\hat{\mathcal{P}})^n\hat{\mathbf{A}}^n$ are properly confined within the subspace $\hat{\mathcal{P}}$, and upon gauge

transformation, all light-matter interaction operators are now consistently confined in $\hat{\mathcal{P}}$ for both gauges. Here, $\hat{\mathcal{U}}$ is defined analogously to the PZW gauge operator $\hat{U}$ in the full space (Eq. 5), and $\hat{\mathcal{P}}\hat{\boldsymbol{\mu}}\hat{\mathcal{P}} \equiv \tilde{\boldsymbol{\mu}}(\hat{\mathbf{x}}, \hat{\mathbf{p}})$ in principle is a function of both $\hat{\mathbf{x}}$ and $\hat{\mathbf{p}}$, due to the finite level projection that ruins the locality of $\hat{\mathbf{x}}$[31,62]. Further, $\hat{\mathcal{U}}$ is a unitary transformation operator in the $\hat{\mathcal{P}}$ subspace and the identity operator in the subspace of $\hat{\mathbb{1}}_{\mathrm{r}} - \hat{\mathcal{P}}$, such that we still have $\hat{\mathcal{U}}\hat{\mathcal{U}}^\dagger = \hat{\mathbb{1}}_{\mathrm{r}} \otimes \hat{\mathbb{1}}_{\mathrm{R}} \otimes \hat{\mathbb{1}}_{\mathrm{ph}} = \hat{U}\hat{U}^\dagger$. Using $\hat{\mathcal{U}}$, one can define the following Coulomb gauge Hamiltonian[36]

$$\hat{\mathcal{H}}_{\mathrm{p\cdot A}} = \hat{\mathcal{U}}^\dagger \hat{\mathcal{H}}_{\mathrm{M}} \hat{\mathcal{U}} + \hat{H}_{\mathrm{ph}}, \tag{26}$$

analogously to $\hat{H}_{\mathrm{p\cdot A}}$ in Eq. 6 in the full space. One can then formally show that $\hat{\mathcal{H}}_{\mathrm{p\cdot A}}$ (Eq. 26) and $\hat{\mathcal{H}}_{\mathrm{d\cdot E}}$ (Eq. 23b) are related through $\hat{\mathcal{U}}$ (Eq. 25) as follows $\hat{\mathcal{U}}\hat{\mathcal{H}}_{\mathrm{p\cdot A}}\hat{\mathcal{U}}^\dagger = \hat{\mathcal{H}}_{\mathrm{M}} + \hat{\mathcal{U}}\hat{H}_{\mathrm{ph}}\hat{\mathcal{U}}^\dagger = \hat{\mathcal{H}}_{\mathrm{d\cdot E}}$. Note that to establish the last equality, we have used the fact that $\hat{\mathcal{U}}\hat{H}_{\mathrm{ph}}\hat{\mathcal{U}}^\dagger = \hat{\mathcal{U}}(\frac{1}{2}\omega_{\mathrm{c}}^2\hat{q}_{\mathrm{c}}^2 + \frac{1}{2}\hat{p}_{\mathrm{c}}^2)\hat{\mathcal{U}}^\dagger = \frac{1}{2}\omega_{\mathrm{c}}^2\hat{q}_{\mathrm{c}}^2 + \frac{1}{2}(\hat{p}_{\mathrm{c}} + \sqrt{2\omega_{\mathrm{c}}/\hbar}\hat{\mathcal{P}}\hat{\boldsymbol{\mu}}\hat{\mathcal{P}}\mathbf{A}_0)^2$. Thus, we have formally demonstrated that the gauge ambiguities between the Coulomb and dipole gauge Hamiltonians can be resolved for an arbitrary matter-cavity hybrid system, under the same level of electronic state truncation.

To further present an equivalent yet convenient $\hat{\mathcal{H}}_{\mathrm{p\cdot A}}$ for molecular cavity QED, we use the electronic states associated with the electronic Hamiltonian $\hat{H}_{\mathrm{el}} = \hat{H}_{\mathrm{M}} - \hat{\mathbf{T}}_{\mathbf{R}}$, where $\hat{\mathbf{T}}_{\mathbf{R}}$ is the nuclear kinetic energy. The *adiabatic* electronic states $|\alpha(\mathbf{R})\rangle$ are the eigenstates of $\hat{H}_{\mathrm{el}}$ through $\hat{H}_{\mathrm{el}}|\alpha(\mathbf{R})\rangle = (\hat{\mathbf{T}}_{\mathbf{r}} + \hat{V})|\alpha(\mathbf{R})\rangle = E_\alpha(\mathbf{R})|\alpha(\mathbf{R})\rangle$. Using $\hat{\mathcal{P}} = \sum_\alpha |\alpha(\mathbf{R})\rangle\langle\alpha(\mathbf{R})|$, the projected electronic Hamiltonian is $\hat{\mathcal{H}}_{\mathrm{el}} = \hat{\mathcal{P}}\hat{H}_{\mathrm{el}}\hat{\mathcal{P}} = \sum_\alpha E_\alpha(\mathbf{R})|\alpha\rangle\langle\alpha|$. Alternatively, diabatic electronic states[63–66] $\{|\varphi\rangle, |\phi\rangle\}$ can be obtained by the unitary transform[63–67] from the adiabatic states $|\alpha(\mathbf{R})\rangle$. The character of the diabatic states do not depend on $\mathbf{R}$, such that $\langle\varphi|\boldsymbol{\nabla}_{\mathbf{R}}|\phi\rangle = 0$. With $\hat{\mathcal{P}} = \sum_\varphi |\varphi\rangle\langle\varphi|$, $\hat{\mathcal{H}}_{\mathrm{el}} = \hat{\mathcal{P}}\hat{H}_{\mathrm{el}}\hat{\mathcal{P}} = \sum_\varphi \mathcal{V}_{\varphi\varphi}(\mathbf{R})|\varphi\rangle\langle\varphi| + \sum_{\varphi\neq\phi}\mathcal{V}_{\varphi\phi}(\mathbf{R})|\varphi\rangle\langle\phi|$, where $\mathcal{V}_{\varphi\phi}(\mathbf{R}) = \langle\varphi|\hat{H}_{\mathrm{el}}|\phi\rangle$ is a diabatic matrix element of $\hat{H}_{\mathrm{el}}$.

By splitting the matter Hamiltonian as $\hat{H}_{\mathrm{M}} = \hat{\mathbf{T}}_{\mathbf{R}} + \hat{H}_{\mathrm{el}}$, then the resulting molecular QED Hamiltonian in this gauge is,

$$\begin{aligned}\hat{\mathcal{H}}_{\mathrm{p\cdot A}} &= \hat{\mathcal{U}}^\dagger\hat{\mathcal{P}}\hat{T}_R\hat{\mathcal{P}}\hat{\mathcal{U}} + \hat{\mathcal{U}}^\dagger\hat{\mathcal{P}}\hat{H}_{\mathrm{el}}(\hat{\mathbf{p}}_r, \hat{\mathbf{x}})\hat{\mathcal{P}}\hat{\mathcal{U}} + \hat{H}_{\mathrm{ph}} \\ &= \sum_{j\in R}\frac{1}{2m_j}\hat{\mathcal{P}}\big(\hat{\mathbf{p}}_j - \boldsymbol{\nabla}_j\tilde{\boldsymbol{\mu}}\hat{\mathbf{A}} + \tilde{\mathbf{P}}_j\big)^2\hat{\mathcal{P}} + \hat{\mathcal{U}}^\dagger\hat{\mathcal{H}}_{\mathrm{el}}\hat{\mathcal{U}} + \hat{H}_{\mathrm{ph}},\end{aligned} \tag{27}$$

where the sum over j *only* includes nuclei, $\tilde{\boldsymbol{\mu}} \equiv \hat{\mathcal{P}}\hat{\boldsymbol{\mu}}\hat{\mathcal{P}}$, and $\tilde{\mathbf{P}}_j$ represents the residue momentum $\tilde{\mathbf{P}}_j \equiv \frac{1}{2}\big(\frac{i}{\hbar}\big)^2[\tilde{\boldsymbol{\mu}}\hat{\mathbf{A}}, [\tilde{\boldsymbol{\mu}}\hat{\mathbf{A}}, \hat{\mathbf{p}}_j]] + ...$ In the above expression, we did not specify the choice of $\hat{\mathcal{P}}$, which could be either adiabatic or diabatic. Under the limiting case when $\mathbf{A}_0 = 0$ or $\tilde{\boldsymbol{\mu}}\cdot\hat{\mathbf{A}} = 0$, both the $-\boldsymbol{\nabla}_j\tilde{\boldsymbol{\mu}}\hat{\mathbf{A}}$ and $\tilde{\mathbf{P}}_j$ terms become 0, and $\hat{\mathcal{U}}^\dagger = \hat{\mathcal{U}} \to \hat{\mathcal{P}} \otimes \hat{\mathbb{1}}_{\mathrm{R}} \otimes \hat{\mathbb{1}}_{\mathrm{ph}}$. Thus, under a such limit, $\hat{\mathcal{H}}_{\mathrm{p\cdot A}} \to \hat{\mathcal{H}}_{\mathrm{M}} + \hat{H}_{\mathrm{ph}}$; hence, the matter and the cavity becomes decoupled. When using adiabatic states for the truncation, one can show that[66,68] $\hat{\mathcal{P}}\hat{\mathbf{p}}_j^2\hat{\mathcal{P}} = (\hat{\mathbf{p}}_j - i\hbar\sum_{\alpha,\beta}\mathbf{d}_{\alpha\beta}^j|\alpha\rangle\langle\beta|)^2$, where $\mathbf{d}_{\alpha\beta}^j \equiv \langle\alpha|\boldsymbol{\nabla}_j|\beta\rangle$ is the well known derivative couplings. Besides these adiabatic derivative couplings, the light-matter interaction also induced additional "derivative"-type couplings, $-\boldsymbol{\nabla}_j\tilde{\boldsymbol{\mu}}\hat{\mathbf{A}}$ and $\tilde{\mathbf{P}}_j$, regardless of the electronic representation used in constructing $\hat{\mathcal{P}}$. When using the Mulliken-Hush diabatic states[64,69] which are the eigenstates of the $\tilde{\boldsymbol{\mu}} \equiv \hat{\mathcal{P}}\hat{\boldsymbol{\mu}}\hat{\mathcal{P}}$ operator, such that $\tilde{\boldsymbol{\mu}} = \sum_\phi \boldsymbol{\mu}_\phi|\phi\rangle\langle\phi|$, one can prove that $\tilde{\mathbf{P}}_j = 0$ for all nuclei. This is because that $\boldsymbol{\nabla}_j\tilde{\boldsymbol{\mu}} = \sum_\phi \boldsymbol{\nabla}_j\boldsymbol{\mu}_\phi|\phi\rangle\langle\phi|$, thus both $\tilde{\boldsymbol{\mu}}\hat{\mathbf{A}}$ and $[\tilde{\boldsymbol{\mu}}\hat{\mathbf{A}}, \hat{\mathbf{p}}_j]$ become purely diagonal matrices, hence all of the higher order commutators in $\hat{\mathcal{U}}^\dagger\hat{\mathbf{p}}_j\hat{\mathcal{U}}$ become zero, resulting in $\tilde{\mathbf{P}}_j = 0$ for $j \in \mathbf{R}$.

As expected, this Properly Truncated Coulomb Gauge Hamiltonian is now gauge invariant. This leads to equivalent results to the d·E Hamiltonian under the same level of truncation. Additionally, it preserves the favorable Fock state convergence behavior of the Coulomb Gauge Hamiltonian. Consequently, it requires fewer matter and Fock states than either of the Hamiltonians discussed above. This convergence behavior is demonstrated numerically in Fig. 4(e) for the Shin-Metiu molecular model.

C. Polarized Fock-State Hamiltonian

The Polarized Fock-State Hamiltonian takes advantage of the disappearance of $\tilde{\mathbf{P}}_j$ when the Hamiltonian is expressed in the Mulliken-Hush diabatic basis to form an equivalent Hamiltonian that provides additional physical intuition. In this representation, the matter Hamiltonian can be expressed as

$$\hat{\mathcal{H}}_{\mathrm{M}} = \hat{\mathbf{T}}_{\mathbf{R}} + \sum_\phi V_\phi(\mathbf{R})\,|\phi\rangle\langle\phi| + \sum_{\phi\neq\varphi} V_{\phi\varphi}(\mathbf{R})\,|\phi\rangle\langle\varphi| \tag{28}$$

where $V_\phi(\mathbf{R})$ represents the diabatic potentials, $V_{\phi\varphi}(\mathbf{R})$ represents the diabatic coupling. The PF Hamiltonian in Eqn. 10 under the $|\phi\rangle$ basis is expressed as

$$\begin{aligned}\hat{\mathcal{H}}_{\mathrm{PF}}^{\mathrm{MH}} =& \hat{\mathcal{U}}_\mu^\dagger\hat{\mathcal{H}}_{\mathrm{PF}}\hat{\mathcal{U}}_\mu \\ =& \hat{H}_{\mathrm{M}} + \frac{\hat{p}_{\mathrm{c}}^2}{2} + \sum_\phi \frac{\omega_{\mathrm{c}}^2}{2}\big(\hat{q}_{\mathrm{c}} + q_\phi^0(\mathbf{R})|\phi\rangle\langle\phi|\big)^2,\end{aligned} \tag{29}$$

where $q_\phi^0(\mathbf{R}) = \sqrt{\frac{2}{\hbar\omega_{\mathrm{c}}}}\mathbf{A_0}\cdot\boldsymbol{\mu}_\phi(\mathbf{R})$, $\boldsymbol{\mu}_\phi$ is eigen-dipole value for $|\phi\rangle$, and $\hat{\mathcal{U}}_\mu$ is the unitary operator that changes the basis to the eigenbasis of $\hat{\boldsymbol{\mu}}$. We notice that the photon field is described as displaced Harmonic oscillator that is centered around $-q_\phi^0(\mathbf{R})$. This displacement can be viewed as a *polarization* of the photon field due to the presence of the molecule-cavity coupling, such that the photon field corresponds to a non-zero (hence polarized) vector potential, in contrast to the vacuum photon field.

The interaction term in Eq. 29 is the Hamiltonian of a displaced Harmonic oscillator and has the following eigen relations.

$$\begin{aligned}&\frac{1}{2}\left[\hat{p}_{\rm c}^2+\omega_{\rm c}^2(\hat{q}_{\rm c}+q_\phi^0(\mathbf{R}))^2\right]|n_\phi(\mathbf{R})\rangle \\ &\equiv(\hat{b}_\phi^\dagger\hat{b}_\phi+\frac{1}{2})\hbar\omega_{\rm c}|n_\phi(\mathbf{R})\rangle=\left(n_\phi+\frac{1}{2}\right)\hbar\omega_{\rm c}|n_\phi(\mathbf{R})\rangle,\end{aligned} \tag{30}$$

where the polarized Fock state (PFS) $|n_\phi(\mathbf{R})\rangle \equiv |n_\phi\rangle$ is the Fock state of a displaced Harmonic oscillator, with the displacement $-q_\phi^0 = -\sqrt{\frac{2}{\hbar\omega_{\rm c}}}\mathbf{A_0}\cdot\boldsymbol{\mu}_\phi(\mathbf{R})$ specific to the diabatic state $|\phi\rangle$ such that $|n_\phi\rangle = e^{-i(-q_\phi^0)\hat{p}/\hbar}|n\rangle = e^{iq_\phi^0\hat{p}/\hbar}|n\rangle$, and $n_\phi = 0,1,2...,\infty$ is the quantum number for the PFS. Further, $\hat{b}_\phi^\dagger = (\hat{q}'_\phi + i\hat{p})/\sqrt{2}$ and $\hat{b}_\phi = (\hat{q}'_\phi - i\hat{p})/\sqrt{2}$ are the creation and annihilation operators of the PFS $|n_\phi\rangle$, with the photon field momentum operator $\hat{p}$ and polarized photon field coordinate operator $\hat{q}'_\phi = \hat{q} + q_\phi^0(\mathbf{R})$. Compared to the vacuum's Fock state $|n\rangle$, these PFS depends on the diabatic state (or more generally, the eigenstate of $\tilde{\boldsymbol{\mu}}$) of the molecule, and the position of the nuclei (through the $\mathbf{R}$ dependence in $\boldsymbol{\mu}_\phi(\mathbf{R})$). Due to the electronic state-dependent nature of the polarization, the PFS associated with different electronic diabatic states become non-orthogonal, *i.e.*, $\langle n_\phi|m_\varphi\rangle \neq \delta_{\phi\varphi}$. Under the special case of the atomic cavity QED, the PFS representation reduces to the qubit-shifted Fock basis $\{|n_+\rangle, |m_-\rangle\}$, which has been used to solve the polariton eigen-spectrum for the quantum Rabi model[70–73] throughout the entire range of light-matter coupling and derive the generalized rotating-wave approximation[70,71,74]. These non-orthogonal Fock states and their overlap $\langle m_-|n_+\rangle$ have shown to effectively capture the light-matter interactions in a quantum Rabi model.[70,71]

To express the Hamiltonian in the PFS representation, the PF Hamiltonian (Eq. 29) undergoes a unitary shift operator (similar to a polaron transformation[15]), $\hat{U}_{\rm pol}$ of the form,

$$\hat{\mathcal{U}}_{\rm pol} = \exp\left\{\left[\frac{i}{\hbar}\sum_\phi q_\phi^0(\boldsymbol{R})\,|\phi\rangle\langle\phi|\,\hat{p}_c\right]\right\} \tag{31}$$

such that it unshifts that displaced Harmonic oscillator in Eq. 29 when applied to $\hat{H}_{\rm PF}$. We then have the PFS Hamiltonian as,

$$\begin{aligned}\hat{\mathcal{H}}_{\rm PFS} =&\hat{\mathcal{U}}_{\rm pol}^\dagger\hat{\mathcal{H}}_{\rm PF}^{\rm MH}\hat{\mathcal{U}}_{\rm pol} \\ =&\hat{\mathcal{U}}_{\rm pol}^\dagger\hat{\mathbf{T}}_{\mathbf{R}}\hat{\mathcal{U}}_{\rm pol} \\ &+\sum_{\phi,n_\phi}\left(V_\phi(\mathbf{R})+(n_\phi+\frac{1}{2})\hbar\omega_{\rm c}\right)|\phi,n_\phi\rangle\langle n_\phi,\phi| \\ &+\sum_{n_\phi,m_\varphi,\phi\neq\varphi}\langle m_\varphi|n_\phi\rangle V_{\phi\varphi}(\mathbf{R})|\phi,n_\phi\rangle\langle m_\varphi,\varphi|.\end{aligned} \tag{32}$$

Note that there is a finite coupling between the $|\phi\rangle$ state with n photons and the $|\varphi\rangle$ state with m photons through the $\langle m_\varphi|n_\phi\rangle V_{\phi\varphi}(\mathbf{R})$ term, which is the diabatic electronic coupling $V_{\phi\varphi}(\mathbf{R})$ scaled by the overlap $\langle m_\varphi|n_\phi\rangle$ of the PFS. Thus, instead of having an explicit light-matter interaction term $\omega_{\rm c}\mathbf{A_0}\cdot\hat{\boldsymbol{\mu}}(\hat{a}^\dagger+\hat{a})$ (and the DSE) as shown in Eqn. 10, these interactions are now carried through $\langle m_\varphi|n_\phi\rangle V_{\phi\varphi}(\mathbf{R})$.

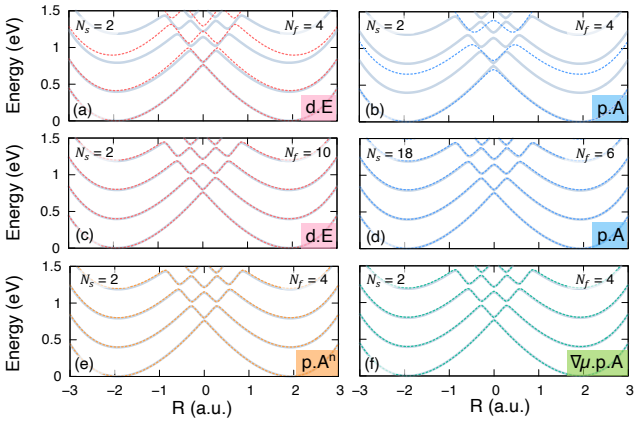

FIG. 4. Comparison of the polariton potential energy surfaces of the Shin-Metiu model generated from four different QED Hamiltonians under different levels of truncation. (a) Pauli-Fierz Hamiltonian with 2 matter states and 4 Fock states. (b) Coulomb gauge Hamiltonian with 2 matter states and 4 Fock states. (c) Pauli-Fierz Hamiltonian with 2 matter states and 10 Fock states. (d) Coulomb gauge Hamiltonian with 18 matter states and 6 Fock states. (e) Properly truncated Coulomb gauge Hamiltonian with 2 matter states and 4 Fock states. (f) Polarized Fock state (PFS) Hamiltonian with 2 matter states and 4 Fock states. This shows how the latter two Hamiltonians require less matter and Fock states to converge compared to the former two.

Further, $\hat{\mathbf{T}}_{\mathbf{R}}$ in this $|\phi,n_\phi\rangle$ basis is given by

$$\hat{\mathcal{U}}_{\rm pol}^\dagger\hat{\mathbf{T}}_{\mathbf{R}}\hat{\mathcal{U}}_{\rm pol} = \frac{1}{2\mathbf{M}}\Big(\hat{\mathbf{P}} - i\hbar\sum_{\phi,n_\phi,m_\phi}\mathbf{d}_{m_\phi n_\phi}|\phi,m_\phi\rangle\langle n_\phi,\phi|\Big)^2, \tag{33}$$

where $\mathbf{d}_{m_\phi n_\phi} = \langle m_\phi|\boldsymbol{\nabla}_{\mathbf{R}}|n_\phi\rangle$ originated from the R-dependence of PFS. Note that there is no non-adiabatic couplings between states with different diabatic characters, since $\langle\phi,n_\phi|\boldsymbol{\nabla}_{\mathbf{R}}|\varphi,m_\varphi\rangle = \langle n_\phi|\boldsymbol{\nabla}_{\mathbf{R}}|m_\varphi\rangle\langle\phi|\varphi\rangle = 0$ (because we assume that $|\phi\rangle$ and $|\varphi\rangle$ are strict diabatic basis), and they are orthogonal $\langle\phi|\varphi\rangle = 0$ for $\phi\neq\varphi$. The polaritonic non-adiabatic coupling can be analytically evaluated as follows

$$\langle m_\phi|\boldsymbol{\nabla}_{\mathbf{R}}|n_\phi\rangle = -\frac{1}{\hbar}\mathbf{A_0}\cdot\boldsymbol{\nabla}_{\mathbf{R}}\boldsymbol{\mu}_\phi(\mathbf{R})\langle\mathbf{m}_\phi|\hat{\mathbf{b}}^\dagger-\hat{\mathbf{b}}|\mathbf{n}_\phi\rangle. \tag{34}$$

Thus, these terms couple off-resonant states that are separated by $\hbar\omega_{\rm c}$ through the $(\hat{b}^\dagger - \hat{b})$ term. This non-adiabatic coupling is reminiscent of the vector potential boost of matter momentum in the Coulomb gauge.

Intuitively, this PFS representation strives to improve the Fock state convergence of the d·E Hamiltonian by us-

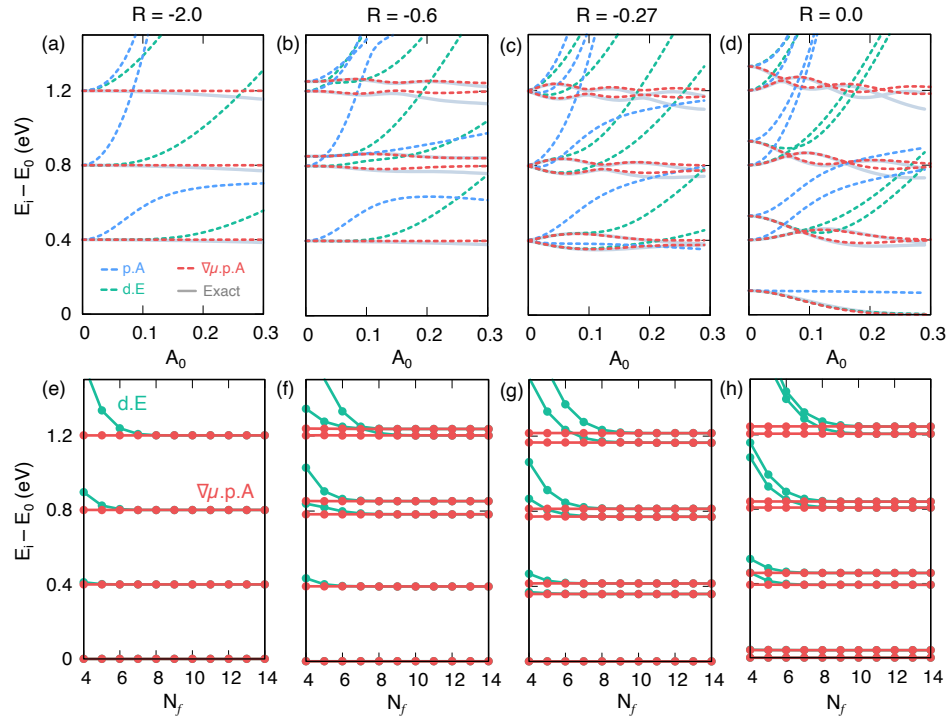

FIG. 5. Comparison of the PFS Hamiltonian (red) energy eigenspectrum with that of the Coulomb (blue) and dipole (green) gauge Hamiltonians for the Shin Metiu model at different R values (denoted at the top of each column). The top panels (a-d) graph the eigenenergies of each Hamiltonian using 2 matter states and 4 Fock states against the exact (grey). The bottom panels (e-h) plot the eigenenergies of the dipole gauge Hamiltonian vs. the PFS Hamiltonian at different R values with an $A_0 = 0.15$ and two matter states as a function of the number of Fock states used.

ing a shifted harmonic oscillator basis instead of the traditional Fock basis of the pure light Hamiltonian. This is because the light-matter coupling itself causes a shift in the photonic Hamiltonian (as shown in Eq. 30). Thus, a shifted harmonic oscillator basis is a more natural basis in which to represent this system. This leads to a significant improvement in Fock state convergence over the d·E Hamiltonian, as shown numerically in Fig. 4. Additionally, Fig. 5 shows in further detail the advantageous convergence properties of the PFS representation compared to $\hat{\mathcal{H}}_{\text{d·E}}$ and $\hat{\mathcal{H}}'_{\text{p·A}}$.

In fact, this PFS representation is equivalent to the properly truncation Coulomb gauge Hamiltonian in Eq. 27. To see this, we first look at how $\hat{U}_\theta$ rotates $\hat{q}_\text{c}$:

$$\hat{U}_\theta^\dagger \hat{q}_\text{c} \hat{U}_\theta = \sqrt{\frac{\hbar}{2\omega_\text{c}}}(\hat{U}_\theta^\dagger \hat{a} \hat{U}_\theta + \hat{U}_\theta^\dagger \hat{a}^\dagger \hat{U}_\theta) = -\frac{\hat{p}_\text{c}}{\omega_\text{c}} \tag{35}$$

This relation directly leads to,

$$\begin{aligned}
\hat{\mathcal{U}}_\mu^\dagger \hat{U}_\theta^\dagger \hat{\mathcal{U}} \hat{U}_\theta \hat{\mathcal{U}}_\mu &= \hat{\mathcal{U}}_\mu^\dagger \hat{U}_\theta^\dagger \exp\left[-\frac{i}{\hbar}\sqrt{\frac{2\omega_\text{c}}{\hbar}}\hat{\boldsymbol{\mu}} \cdot \mathbf{A}_0 \hat{q}_\text{c}\right] \hat{U}_\theta \hat{\mathcal{U}}_\mu \\
&= \hat{\mathcal{U}}_\mu^\dagger \exp\left[\frac{i}{\hbar}\sqrt{\frac{2}{\hbar\omega_\text{c}}}\hat{\boldsymbol{\mu}} \cdot \mathbf{A}_0 \hat{p}_\text{c}\right] \hat{\mathcal{U}}_\mu \\
&= \exp\left[\frac{i}{\hbar}\sum_\phi \sqrt{\frac{2}{\hbar\omega_\text{c}}}\boldsymbol{\mu}_\phi \cdot \mathbf{A}_0 \left|\phi\right\rangle\!\left\langle\phi\right| \hat{p}_\text{c}\right] = \hat{U}_\text{pol}
\end{aligned} \tag{36}$$

With the properties shown in Eqs. 35 and 37, we can directly show that $\hat{\mathcal{H}}_\text{PFS}$ and $\hat{\mathcal{H}}_\text{p·A}$ differ only by a change in basis for the matter Hilbert space and a phase rotation in the photonic Hilbert space by the following relationship:

$$\begin{aligned}
\hat{\mathcal{H}}_\text{PFS} &= \hat{\mathcal{U}}_\text{pol}^\dagger \hat{\mathcal{H}}_\text{PF}^\text{MH} \hat{\mathcal{U}}_\text{pol} = \hat{\mathcal{U}}_\text{pol}^\dagger (\hat{\mathcal{U}}_\mu^\dagger \hat{\mathcal{H}}_\text{PF} \hat{\mathcal{U}}_\mu) \hat{\mathcal{U}}_\text{pol} \\
&= \hat{\mathcal{U}}_\text{pol}^\dagger (\hat{\mathcal{U}}_\mu^\dagger [\hat{U}_\theta^\dagger \hat{\mathcal{H}}_\text{d·E} \hat{U}_\theta] \hat{\mathcal{U}}_\mu) \hat{\mathcal{U}}_\text{pol} \\
&= (\hat{\mathcal{U}}_\mu^\dagger \hat{U}_\theta^\dagger \hat{\mathcal{U}}^\dagger \hat{U}_\theta \hat{\mathcal{U}}_\mu)(\hat{\mathcal{U}}_\mu^\dagger [\hat{U}_\theta^\dagger \hat{\mathcal{H}}_\text{d·E} \hat{U}_\theta] \hat{\mathcal{U}}_\mu)(\hat{\mathcal{U}}_\mu^\dagger \hat{U}_\theta^\dagger \hat{\mathcal{U}} \hat{U}_\theta \hat{\mathcal{U}}_\mu) \\
&= \hat{\mathcal{U}}_\mu^\dagger \hat{U}_\theta^\dagger \hat{\mathcal{U}}^\dagger \hat{\mathcal{H}}_\text{d·E} \hat{\mathcal{U}} \hat{U}_\theta \hat{\mathcal{U}}_\mu \\
&= \hat{\mathcal{U}}_\mu^\dagger \hat{U}_\theta^\dagger \hat{\mathcal{H}}_\text{p·A} \hat{U}_\theta \hat{\mathcal{U}}_\mu
\end{aligned} \tag{37}$$

Note that $[\hat{U}_\theta, \hat{\mathcal{U}}_\mu] = 0$ since they act on different degrees of freedom. In this way, $\hat{\mathcal{H}}_\text{PFS}$ and $\hat{\mathcal{H}}_\text{p·A}$ are intrinsically related. It follows naturally that they would have very similar convergence properties. Consequentially, in the full basis limit, the PFS representation is equivalent to the p·A Hamiltonian. This is shown in the following section.

Figure 2 summarizes the relationships between all the Hamiltonians discussed thus far.

D. Truncation of Photonic Mode for the Coulomb and Dipole Gauges

All the Hamiltonians previously discussed in this review are under the single mode approximation; however, many types of cavities such as the Fabry–Pérot cavity has a infinite number of quantized modes (see Sect. VI). It is then pertinent to consider how to truncate this many-mode Hilbert space to a more computable space with a small finite number of modes. Whenever a truncation occurs, the gauge invariance condition may become ambiguous.

Although less ubiquitous than the gauge ambiguities present under matter truncation, it should be noted that the truncation of photonic modes also leads to gauge ambiguities that can be resolved in a manner similar to the process discussed in Sect. III B[75]. However, unlike in the case of matter truncation, for mode truncation, the dipole gauge Hamiltonian leads to ambiguities. To see this, recall how $\hat{H}_{\text{p·A}}$ and $\hat{H}_{\text{d·E}}$ can be written in terms of the PZW operator.

$$\hat{H}_{\text{p·A}} = \hat{U}^\dagger \hat{H}_{\text{M}} \hat{U} + \hat{H}_{\text{ph}} \tag{38}$$

$$\hat{H}_{\text{d·E}} = \hat{H}_{\text{M}} + \hat{U} \hat{H}_{\text{ph}} \hat{U}^\dagger; \tag{39}$$

however, now $\hat{H}_{\text{ph}} = \sum_{k=0}^{\infty} \hbar\omega_k \hat{a}_k^\dagger \hat{a}_k$, where $\hat{a}_k$ is the photonic annihilation operator for the k_{th} mode.

It is convenient to define a projection operator, $\hat{\mathcal{P}}^{(m)}$, that truncates this many-mode Hilbert space to an m-mode Hilbert space.

$$\hat{\mathcal{P}}^{(m)} = \hat{\mathcal{I}}_{\text{M}} \otimes \Big(\bigotimes_{k=0}^{m-1} \sum_{n=0}^{\infty} |n_k\rangle\langle n_k| \bigotimes_{k'=m}^{\infty} |0_{k'}\rangle\langle 0_{k'}| \Big), \tag{40}$$

where $|n_k\rangle$ is the n_{th} Fock state in the k_{th} mode and $\hat{\mathcal{I}}_M$ is the identity operator for the matter Hilbert space.

For the case of matter truncation, it was argued that to properly truncate polariton systems in a truncated subspace, the pure matter and photonic operators should be truncated first and then transformed with a properly truncated PZW operator. As discussed in Ref. 75, the same procedure must be used for mode truncation. In this manner, the new m-mode PZW operator is,

$$\hat{\mathcal{U}}^{(m)} = e^{-\frac{i}{\hbar}\hat{\mathcal{P}}^{(m)}(\hat{\boldsymbol{\mu}}\cdot\hat{\boldsymbol{A}})\hat{\mathcal{P}}^{(m)}} = \exp\left[-\frac{i}{\hbar}\hat{\boldsymbol{\mu}} \cdot \sum_{k=0}^{m-1} \boldsymbol{A}_k (\hat{a}_k^\dagger + \hat{a}_k) \right]. \tag{41}$$

Now, if we formulate the equivalents to Eqs. 38-39 in this m-mode subspace as,

$$\hat{\mathcal{H}}_{\text{p·A}} = \hat{\mathcal{U}}^\dagger \hat{\mathcal{P}} \hat{H}_{\text{M}} \hat{\mathcal{P}} \hat{\mathcal{U}} + \hat{\mathcal{P}} \hat{H}_{\text{ph}} \hat{\mathcal{P}} \tag{42}$$

$$\hat{\mathcal{H}}_{\text{d·E}} = \hat{\mathcal{P}} \hat{H}_{\text{M}} \hat{\mathcal{P}} + \hat{\mathcal{U}} \hat{\mathcal{P}} \hat{H}_{\text{ph}} \hat{\mathcal{P}} \hat{\mathcal{U}}^\dagger, \tag{43}$$

which always guarantees gauge invariant results through $\hat{\mathcal{H}}_{\text{d·E}} = \hat{\mathcal{U}} \hat{\mathcal{H}}_{\text{p·A}} \hat{\mathcal{U}}^\dagger$. Now, we can find the Coulomb gauge Hamiltonian under an m-mode truncation by using Eq. 42:

$$\begin{aligned} \hat{\mathcal{H}}_{\text{p·A}}^{(m)} &= \hat{\mathcal{U}}^{(m)\dagger} \hat{\mathcal{P}}^{(m)} \hat{H}_{\text{M}} \hat{\mathcal{P}}^{(m)} \hat{\mathcal{U}}^{(m)} + \hat{\mathcal{P}}^{(m)} \sum_{k=0}^{\infty} \hbar\omega_k \hat{a}_k^\dagger \hat{a}_k \hat{\mathcal{P}}^{(m)} \\ &= \hat{H}_{\text{M}} + \sum_{k=0}^{m-1} \Big[\hbar\omega_k \hat{a}_k^\dagger \hat{a}_k + \frac{\hat{\boldsymbol{p}} \cdot \boldsymbol{A}_k}{m} (\hat{a}_k^\dagger + \hat{a}_k) \Big] \\ &\quad + \frac{1}{2m} \Big[\sum_{k=0}^{m-1} |\boldsymbol{A}_k| (\hat{a}_k^\dagger + \hat{a}_k) \Big]^2. \end{aligned} \tag{44}$$

Since $\hat{H}_{\text{M}}$ is a pure matter operator, it is invariant upon mode truncation and therefore commutes with $\hat{\mathcal{P}}$, $\hat{\mathcal{P}}^{(m)} \hat{H}_{\text{M}} \hat{\mathcal{P}}^{(m)} = \hat{H}_{\text{M}} \hat{\mathcal{P}}^{(m)}$. In the case of a single mode $m = 1$, Eq. 44 reduces to the well-known single-mode minimal coupling Hamiltonian (see Eq. 4). Interestingly, if we apply a simple mode truncation, $\hat{\mathcal{H}}_{\text{p·A}}^{\prime(m)} = \hat{\mathcal{P}}^{(m)} \hat{H}_{\text{p·A}} \hat{\mathcal{P}}^{(m)}$ has the same form of Eq. 44 up to a constant that represents the zero-point energy of all modes.

Since the minimal coupling Hamiltonian is formed by boosting the matter Hamiltonian, a naive mode truncation has a minimal effect, only causing a zero-point energy (ZPE) shift.

$$\begin{aligned} \hat{\mathcal{H}}_{\text{p·A}}^{\prime(m)} &= \hat{\mathcal{P}}^{(m)} \hat{H}_{\text{p·A}} \hat{\mathcal{P}}^{(m)} \\ &= \hat{\mathcal{P}}^{(m)} \hat{U}^\dagger \hat{H}_{\text{M}} \hat{U} \hat{\mathcal{P}}^{(m)} + \hat{\mathcal{P}}^{(m)} \sum_{k=0}^{\infty} \hbar\omega_k \hat{a}_k^\dagger \hat{a}_k \hat{\mathcal{P}}^{(m)} \\ &= \hat{H}_{\text{M}} + \sum_{k=0}^{m-1} \left[\hbar\omega_k \hat{a}_k^\dagger \hat{a}_k + \frac{\hat{\boldsymbol{p}} \cdot \boldsymbol{A}_k}{m} (\hat{a}_k^\dagger + \hat{a}_k) \right] \\ &\quad + \frac{1}{2m} \left[\sum_{k=0}^{m-1} |\boldsymbol{A}_k| (\hat{a}_k^\dagger + \hat{a}_k) \right]^2 + \mathcal{E} \hat{\mathcal{P}}^{(m)}, \end{aligned} \tag{45}$$

where $\mathcal{E} = \sum_{k=n}^{\infty} |\boldsymbol{A}_k|^2 / 2m$ is ZPE of the other projected modes coming from $\hat{\mathcal{P}}^{(m)} (\hat{a}_k^\dagger + \hat{a}_k)^2 \hat{\mathcal{P}}^{(m)} = \hat{\mathcal{P}}^{(m)}$ for $k \geq m$ (note that the only surviving term is $\hat{\mathcal{P}}^{(m)} \hat{a}_k \hat{a}_k^\dagger \hat{\mathcal{P}}^{(m)} = \hat{\mathcal{P}}^{(m)}$). This is very different from what happens in the case of a matter truncation.

Now, the Hamiltonian that fails under a simple mode truncation is the dipole gauge Hamiltonian.

$$\begin{aligned} \hat{\mathcal{H}}_{\text{d·E}}^{\prime(m)} &= \hat{\mathcal{P}}^{(m)} \hat{H}_{\text{d·E}} \hat{\mathcal{P}}^{(m)} \\ &= \hat{H}_{\text{M}} + \hat{\mathcal{P}}^{(m)} \hat{U} \big(\sum_{k=0}^{\infty} \hbar\omega_k \hat{a}_k^\dagger \hat{a}_k \big) \hat{U}^\dagger \hat{\mathcal{P}}^{(m)} \\ &= \hat{H}_{\text{M}} + \sum_{k=0}^{m-1} \left[\hbar\omega_k \hat{a}_k^\dagger \hat{a}_k + i\omega_k \boldsymbol{A}_k \cdot \hat{\boldsymbol{\mu}} (\hat{a}_k^\dagger - \hat{a}_k) \right] \\ &\quad + \sum_{k=0}^{\infty} \frac{\omega_k}{\hbar} (\boldsymbol{A}_k \cdot \hat{\boldsymbol{\mu}})^2. \end{aligned} \tag{46}$$

This procedure breaks the gauge invariance and generate different results from $\hat{\mathcal{H}}_{\text{p·A}}^{(m)}$, because the dipole self-energies for all the modes are still explicitly present, even

for the modes $k \in [m, \infty]$ which are supposed to be projected away. Thus, the dipole gauge Hamiltonian should be truncated using the scheme presented in Eq. 43,

$$\hat{\mathcal{H}}^{(m)}_{\mathrm{d.E}} = \hat{H}_{\mathrm{M}} + \hat{\mathcal{U}}^{(m)}\hat{\mathcal{P}}^{(m)}\Big(\sum_{k=0}^{\infty}\hbar\omega_k\hat{a}_k^\dagger\hat{a}_k\Big)\hat{\mathcal{P}}^{(m)}\hat{\mathcal{U}}^{(m)\dagger} \tag{47}$$

$$=\hat{H}_{\mathrm{M}} + \sum_{k=0}^{n-1}\left[\hbar\omega_k\hat{a}_k^\dagger\hat{a}_k + i\omega_k\boldsymbol{A}_k\cdot\hat{\boldsymbol{\mu}}(\hat{a}_k^\dagger - \hat{a}_k) + \frac{\omega_k}{\hbar}(\boldsymbol{A}_k\cdot\hat{\boldsymbol{\mu}})^2\right].$$

This provides gauge invariant results with Eq. 45 and reduces to the well-known single mode case (see Eq. 7) when $m = 1$. In this manner, one should carefully consider the proper manner of truncation even for mode truncation.

E. Generalization of Truncation Scheme Beyond the Long-Wavelength Approximation

In recent work[76], a generalized scheme for resolving gauge ambiguities beyond the long-wavelength approximation and for arbitrary gauges. In this picture, the matter is no longer approximated as a dipole and instead must be described as a charge density function, $\rho(\mathbf{x})$,

$$\hat{\rho}(\mathbf{x}, \{\hat{\mathbf{r}}_j\}) = \sum_j q_j\delta(\mathbf{x} - \hat{\mathbf{r}}_j), \tag{48}$$

where j indexes over all charged particles of charge q_j and position $\hat{\mathbf{r}}_j$ and $\mathbf{x}$ is the global Cartesian coordinate system. This charge density function is used to fix the longitudinal (curl-free) component of the auxiliary polarization field, $\hat{\mathbf{P}}^g(\mathbf{x}, \{\hat{\mathbf{r}}_j\})$, such that

$$\hat{\nabla}\cdot\hat{\mathbf{P}}^g(\mathbf{x}, \{\hat{\mathbf{r}}_j\}) = -\hat{\rho}(\mathbf{x}, \{\hat{\mathbf{r}}_j\}), \tag{49}$$

and the transverse (divergence-free) component must be defined for a given gauge, g. For example, in the Coulomb gauge, $\hat{\mathbf{P}}^{\mathrm{C}}_\perp = 0$ and in the multi-polar gauge (the dipole gauge beyond the long-wavelength approximation), $\hat{\mathbf{P}}^{\mathrm{mp}}_\perp = \sum_j q_j\hat{\mathbf{r}}_j\int_0^1 ds\ \delta_\perp(\mathbf{x} - s\hat{\mathbf{r}}_j)$.

To transform between gauges, a more generalized gauge transformation in terms of the polarization fields is needed.

$$\hat{W}_{g\to g'} = \exp\left[\frac{i}{\hbar}\int d\mathbf{x}\ \left[\hat{\mathbf{P}}^{g'}_\perp - \hat{\mathbf{P}}^{g}_\perp\right]\cdot\hat{\boldsymbol{A}}(\mathbf{x})\right], \tag{50}$$

where $\hat{W}_{g\to g'}$ is a unitary operator that transforms an operator from the gauge, g, to the gauge, g', $\hat{\boldsymbol{A}}(\mathbf{x})$ is once again the transverse component of the vector potential, the explicit $\mathbf{x}, \{\hat{\mathbf{r}}_j\}$ dependence is not written for brevity.

With this formalism, the light-matter Hamiltonian in an arbitrary gauge, $\hat{H}_g$, can now be written as

$$\hat{H}_g = \hat{W}_{\mathrm{C}\to g}\hat{H}_{\mathrm{M}}\hat{W}^\dagger_{\mathrm{C}\to g} + \hat{W}_{\mathrm{mp}\to g}\hat{H}_{\mathrm{ph}}\hat{W}^\dagger_{\mathrm{mp}\to g}, \tag{51}$$

Under the long-wavelength approximation, this result reduces to the relations shown in Eqs. 38 and 39. Similar to the previous sections under the long-wavelength approximation, transforming $g \to g'$ follows the simple relation $\hat{H}_{g'} = \hat{W}_{g\to g'}\hat{H}_g\hat{W}_{g\to g'}$.

To resolve gauge ambiguities upon truncation, a similar process to the previous sections is performed. First, the pure matter and the pure photonic Hamiltonians are projected, $H_{\mathrm{M}} \to \mathcal{H}_{\mathrm{M}}$ and $H_{\mathrm{ph}} \to \mathcal{H}_{\mathrm{ph}}$.

Then, the unitary operator, $\hat{W}_{g\to g'}$ is properly confined in the truncated subspace. For the matter DOFs, the argument in the exponential of $\hat{W}_{g\to g'}$ is no longer given to be linear with $\{\mathbf{r}_j\}$ with the relaxation of the long-wavelength approximation. Due to this, the argument of the exponential cannot be directly projected by $\hat{\mathcal{P}}$. Instead, $\hat{W}_{g\to g'}$ must be represented in terms of $\hat{\mathbf{r}}_j = \hat{\mathcal{P}}\hat{\mathbf{r}}_j\hat{\mathcal{P}}$. In this manner, the polarization field is projected in terms of $\{\hat{\mathbf{r}}_j\}$ such that $\hat{\mathbf{P}}^g(\mathbf{x}, \{\hat{\mathbf{r}}_j\}) \to \hat{\boldsymbol{\mathcal{P}}}^g(\mathbf{x}, \{\hat{\mathbf{r}}_j\})$. For the photonic DOFs, the mode truncation in this regime is done in the same fashion as in the previous section, where the vector potential is directly projected as $\hat{\boldsymbol{A}}(\mathbf{x}) \to \hat{\mathcal{P}}\hat{\boldsymbol{A}}(\mathbf{x})\hat{\mathcal{P}} = \hat{\boldsymbol{\mathcal{A}}}(\mathbf{x})$. The gauge transformation in the properly confined in the truncated subspace can then be written as

$$\hat{\mathcal{W}}_{g\to g'} = \exp\left[\frac{i}{\hbar}\int d\mathbf{x}\ \left[\hat{\boldsymbol{\mathcal{P}}}^{g'}_\perp - \hat{\boldsymbol{\mathcal{P}}}^{g}_\perp\right]\cdot\hat{\boldsymbol{\mathcal{A}}}(\mathbf{x})\right], \tag{52}$$

where the $(\mathbf{x}, \{\hat{\mathbf{r}}_j\})$ dependence in $\hat{\boldsymbol{\mathcal{P}}}^g_\perp$ is suppressed for brevity.

Finally, the gauge invariant Hamiltonian for an arbitrary gauge, g, can be constructed using the properly confined gauge transformation, $\hat{\mathcal{W}}_{g\to g'}$, as

$$\hat{\mathcal{H}}_g = \hat{\mathcal{W}}_{\mathrm{C}\to g}\hat{\mathcal{H}}_{\mathrm{M}}\hat{\mathcal{W}}^\dagger_{\mathrm{C}\to g} + \hat{\mathcal{W}}_{\mathrm{mp}\to g}\hat{\mathcal{H}}_{\mathrm{ph}}\hat{\mathcal{W}}^\dagger_{\mathrm{mp}\to g}. \tag{53}$$

In this manner, even beyond the long-wavelength approximation, gauge ambiguities can be resolved by carefully representing all operators in terms of truncated coordinate and momentum operators. In Ref.[76], the formal derivation of this method in the context of macroscopic QED is provided at length.

IV. MODEL HAMILTONIANS IN QUANTUM OPTICS

In quantum optics, a two-level atom coupled to a single mode in an optical cavity is a well-studied subject. This leads to well-known model Hamiltonians, such as the Rabi model and the Jaynes-Cummings model. Since these two models are also widely used in recent investigations of polariton chemistry, here we briefly derive them from the PF Hamiltonian.

We consider a molecule with two electronic states

$$\hat{\mathcal{H}}_{\mathrm{M}} = \hat{T} + E_g(R)|g\rangle\langle g| + E_e(R)|e\rangle\langle e|, \tag{54}$$

and the transition dipole is $\boldsymbol{\mu}_{eg} = \langle e|\hat{\boldsymbol{\mu}}|g\rangle$. Note that the permanent dipoles in a molecule $\boldsymbol{\mu}_{ee} = \langle e|\hat{\boldsymbol{\mu}}|e\rangle$, $\boldsymbol{\mu}_{gg} =$

$\langle g|\hat{\boldsymbol{\mu}}|g\rangle$ are not necessarily zero, as opposed to the atomic case where they are always zero. Hence, it is not always a good approximation to drop them.

The Rabi model, however, assumes that one can ignore the permanent dipole moments (PDM) and leads to the dipole operator expression in the subspace $\hat{\mathcal{P}} = |g\rangle\langle g| + |e\rangle\langle e|$ of

$$\hat{\mathcal{P}}\hat{\boldsymbol{\mu}}\hat{\mathcal{P}} = \boldsymbol{\mu}_{eg}(|e\rangle\langle g| + |g\rangle\langle e|) \equiv \boldsymbol{\mu}_{eg}(\hat{\sigma}^\dagger + \hat{\sigma}), \tag{55}$$

where we have defined the creation operator $\hat{\sigma}^\dagger \equiv |e\rangle\langle g|$ and annihilation operator $\hat{\sigma} \equiv |g\rangle\langle e|$ of the electronic excitation. The PF Hamiltonian (Eq. 10) in the subspace $\hat{\mathcal{P}}$ thus becomes

$$\hat{\mathcal{H}}_{\text{noPDM}} = \hat{\mathcal{H}}_{\text{M}} + \hat{H}_{\text{ph}} + \omega \boldsymbol{A}_0 \cdot \boldsymbol{\mu}_{eg}(\hat{\sigma}^\dagger + \hat{\sigma})(\hat{a}^\dagger + \hat{a}) + \omega(\boldsymbol{A}_0 \cdot \boldsymbol{\mu}_{eg})^2. \tag{56}$$

Dropping the DSE (the last term) from Eq. 56 leads to the Rabi Model

$$\hat{\mathcal{H}}_{\text{Rabi}} = \hat{\mathcal{H}}_{\text{M}} + \hat{H}_{\text{ph}} + \omega \boldsymbol{A}_0 \cdot \boldsymbol{\mu}_{eg}(\hat{\sigma}^\dagger + \hat{\sigma})(\hat{a}^\dagger + \hat{a}). \tag{57}$$

Dropping both the DSE and the counter-rotating terms $\hat{\sigma}^\dagger\hat{a}^\dagger$ and $\hat{\sigma}\hat{a}$ leads to the well-known Jaynes-Cummings (JC) Model[77] as follows

$$\hat{\mathcal{H}}_{\text{JC}} = \hat{\mathcal{H}}_{\text{M}} + \hat{H}_{\text{ph}} + \omega \boldsymbol{A}_0 \cdot \boldsymbol{\mu}_{eg}(\hat{\sigma}^\dagger\hat{a} + \hat{\sigma}\hat{a}^\dagger). \tag{58}$$

This Jaynes-Cummings Hamiltonian is used ubiquitously across the field of quantum optics, from quantum computing[78] applications to fundamental physics experiments[79,80]. For experimentalists and theorists alike, this well-established Hamiltonian is appealing due to its simplicity and intuitive physical interpretation. Eq. 58 can be broken down and interpreted in four parts: $\hat{\mathcal{H}}_{\text{M}}$ is the pure matter Hamiltonian, $\hat{H}_{\text{ph}}$ is the pure light Hamiltonian, $\omega \boldsymbol{A}_0 \cdot \boldsymbol{\mu}_{eg}\hat{\sigma}^\dagger\hat{a}$ represents absorption of a photon of energy ω, and $\omega \boldsymbol{A}_0 \cdot \boldsymbol{\mu}_{eg}\hat{\sigma}\hat{a}^\dagger$ represents emission of a photon of energy ω. While in many cases this is a convenient and adequate Hamiltonian for weak coupling strengths, in chemically relevant coupling strengths (strong coupling and beyond), this Jaynes-Cummings Hamiltonian is no longer adequate.

To demonstrate the limitations due to the series of approximations in the Jaynes-Cummings Hamiltonian, we compare it to three other two-level system Hamiltonians to isolate the effect of a given approximation on the accuracy of the polaritonic eigenspectrum. Namely, we will compare it to the Rabi Hamiltonian, the PF Hamiltonian without PDM (Eq. 56), and introduce a two-level Pauli-Fierz Hamiltonian without DSE,

$$\hat{\mathcal{H}}_{\text{noDSE}} = \hat{\mathcal{H}}_{\text{M}} + \hat{H}_{\text{ph}} + \omega \boldsymbol{A}_0 \cdot \hat{\boldsymbol{\mu}}(\hat{a}^\dagger + \hat{a}). \tag{59}$$

In Fig. 6, $\hat{\mathcal{H}}_{\text{noPDM}}$ and $\hat{\mathcal{H}}_{\text{noDSE}}$ are compared to the Rabi and JC models. This helps explain which approximations lead to the various errors in the JC Hamiltonian eigenspectrum, and provides some insight into why the JC Hamiltonian tends to outperform the Rabi Hamiltonian even though the former has more approximations.

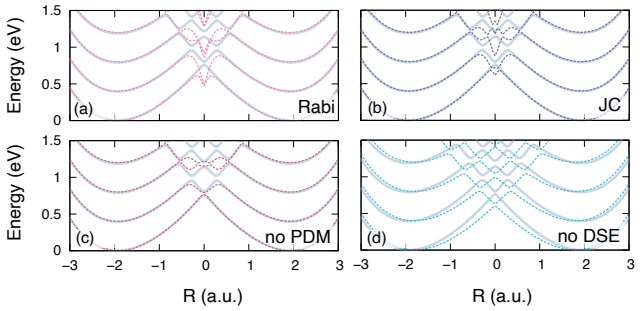

FIG. 6. Comparison of the polariton potential energy surfaces of the Shin-Metiu model generated from four different quantum optics model Hamiltonians with the full Pauli-Fierz Hamiltonian plotted in the light gray lines. (a) Rabi Hamiltonian. (b) Jaynes-Cummings (JC) Hamiltonian. (c) Two-level Pauli-Fierz Hamiltonian without the permanent dipole moments (PDM). (d) Pauli-Fierz Hamiltonian without the dipole self-energy (DSE).

Compared to the more rigorous two-level PF Hamiltonian, the JC Hamiltonian makes three additional approximations: the neglection of DSE, the removal of PDM, and the rotating-wave approximation.

As shown in Fig. 6(c), the removal of PDM leads to an increase in the splitting at the various avoided crossings. Then, removing the DSE (in panel (d)) causes a uniform, R-dependent downward shift for all states. The combination of these approximations gives the Rabi model, as seen in panel (a). The JC model comes from applying the RWA on the Rabi model. By comparing panels (a) and (b), we see that the RWA cancels some of the errors induced by neglecting the DSE. Due to this partial cancellation of errors, the JC model indeed provides more accurate eigenspectra than the Rabi model in many cases.

V. CONNECTION AND DIFFERENCE WITH THE FLOQUET THEORY

While this review focuses on cavity QED, another popular method for modeling light-matter interactions is Floquet theory. For the sake of clarity, in this section, we will briefly introduce Floquet theory and contrast it with cavity QED to provide context as to the use cases for each.

We start our analysis by expanding the minimal coupling Hamiltonian in the Coulomb gauge from Eq. 4 for a single electron ($m = 1$) in a potential,

$$\hat{H}_{\text{p}\cdot\text{A}} = \hat{H}_{\text{M}} - \hat{\mathbf{p}} \cdot \hat{\mathbf{A}} + \hat{\mathbf{A}}^2 + \hat{H}_{\text{ph}}, \tag{60}$$

where in cavity QED, $\hat{\mathbf{A}} = \boldsymbol{e}A_0(\hat{a}^\dagger + \hat{a})$ is proportional to the coordinate operator for a quantum harmonic oscillator. Fig. 7(b) shows the structure of this Hamiltonian in its matrix formalism.

Typically, Floquet theory is used to describe laser-driven systems, and treats the light field classically (the

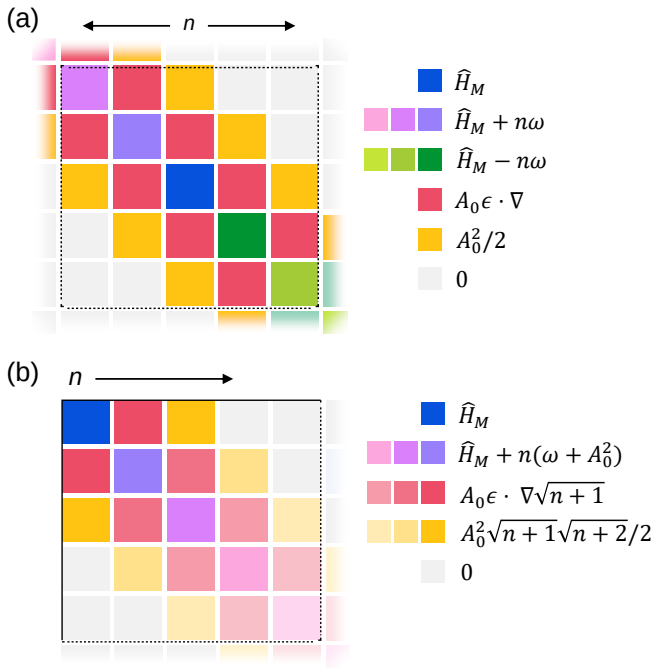

FIG. 7. **Comparison with Floquet Theory:** Comparison of the matrix formulation for (a) the time-dependent Schrödinger equation with Floquet theory from Eq. 63 and (b) time-independent Schrödinger equation with the Coulomb Gauge Hamiltonian.[81]

infinite photon limit). Following the formalism of Ref. 81, $\hat{H}_{\text{ph}}$ is ignored and $\hat{\mathbf{A}} \rightarrow \mathbf{A}(t) = 2A_0\boldsymbol{e}\sin(\omega t)$ is now the classical vector potential for a monochromatic plane wave. The resulting Hamiltonian becomes,

$$\begin{aligned}\hat{H}^{\text{F}}_{\text{p·A}}(t) =& \hat{H}_{\text{M}} + A_0^2 - \hbar\boldsymbol{\nabla}\cdot\boldsymbol{e}A_0(e^{i\omega t} - e^{-i\omega t}) \\ &+ \frac{A_0^2}{2}(e^{2i\omega t} + e^{-2i\omega t}),\end{aligned} \tag{61}$$

where $\hat{\mathbf{p}} = -i\hbar\boldsymbol{\nabla}$ and the A_0^2 term is just a zero point energy that will be ignored going forward. Since in this perspective light is just a classical, oscillating electromagnetic field with perfect periodicity, a time analog to Bloch's theorem can be used to express a state that satisfies the time-dependent Schrödinger equation, $\left|\Psi_\alpha(t)\right\rangle$, in terms of static states, $\left|\psi_n^\alpha\right\rangle$ as,

$$\left|\Psi_\alpha(t)\right\rangle = e^{-iE_\alpha t}\sum_{n=-\infty}^{\infty} e^{in\omega t}\left|\psi_n^\alpha\right\rangle, \tag{62}$$

where α indexes over the Floquet states, E_α is a quasienergy, and ω is the driving frequency of the EM field[82]. Using Eqs. 61-62, the time-dependent Schrödinger equation in the Sambe space[83] can be written as,

$$\begin{aligned}E_\alpha\left|\Psi_\alpha(t)\right\rangle = \sum_{n=-\infty}^{\infty}\Big[&\left(\hat{H}_{\text{M}} + n\hbar\omega\right)e^{in\omega t} \\ &+ \hbar\boldsymbol{\nabla}\cdot\boldsymbol{e}A_0\left(e^{i(n+1)\omega t} - e^{i(n-1)\omega t}\right) \\ &- \frac{A_0^2}{2}\left(e^{i(n+2)\omega t} + e^{i(n-2)\omega t}\right)\Big]\left|\psi_n^\alpha\right\rangle.\end{aligned} \tag{63}$$

The right hand side of this equation is an operator whose structure is visualized in Fig. 7(a) with each block corresponding to a given n. The first term of Eq. 63 corresponds to the diagonal blocks, the second term corresponds the light green off-diagonal blocks, and the third term corresponds the light blue off-diagonal blocks.

It should be noted that this analysis is done in the Coulomb gauge. A similar derivation can be done in the dipole gauge, creating a Floquet equivalent to the PF Hamiltonian shown in Eq. 10. The time-dependent Schrödinger equation can then be written as,

$$\begin{aligned}E_\alpha\left|\Psi_\alpha(t)\right\rangle = \sum_{n=-\infty}^{\infty}\Big[&\left(\hat{H}_{\text{M}} + \frac{\hbar}{\omega}(A_0\boldsymbol{e}\cdot\hat{\boldsymbol{\mu}})^2 + n\hbar\omega\right)e^{in\omega t} \\ &- A_0\hat{\boldsymbol{\mu}}\cdot\boldsymbol{e}\left(e^{i(n+1)\omega t} + e^{i(n-1)\omega t}\right)\Big]\left|\psi_n^\alpha\right\rangle.\end{aligned} \tag{64}$$

Because there is no $\mathbf{A}(t)^2$ term in this Hamiltonian, this Hamiltonian is tridiagonal in the photonic DOF. This significantly decreases the number of n blocks needed to converge eigenspectrum of this Hamiltonian, making this form more popular for modelling laser-driven systems. A detailed matrix form of the Floquet Hamiltonian can be found in Ref. 84, Chapter 9 (see Fig. 9.5).

Fundamentally, Floquet theory depends on the assumption that the light field is strong enough that the photon number is reaching the infinite limit. In that limit, the matrix structure of Fig. 7(a) converges to that of Fig. 7(b) upon rescaling A_0 and subtracting a zero point energy. As discussed in Ref. 85, the Floquet picture in this limit can be thought of as the QED Hamiltonian when considering a range of Fock states that are sufficiently highly excited such that $\sqrt{n} \approx \sqrt{n+\delta n}$, where δn is the number of Floquet blocks considered. Thus, under this limit of an intense field interacting with the matter, Floquet theory is a natural choice for strongly driven systems since numerical convergence can be reached for a few Floquet blocks. However, in the few photon limit, Floquet theory does break down, and the explicit QED treatment is necessary. It also suggests that the fundamental difference between the Floquet picture and the QED picture arises in the few photon limits. For example, when the hybrid system quickly explores several photon-dressed states $|g, n+1\rangle \rightarrow |e, n\rangle$ through light-matter coupling and $|e, n\rangle \rightarrow |g, n\rangle$ through non-adiabatic coupling $\langle e|\nabla|g\rangle$, the system will explore the

different photon number blocks, and the light-matter coupling strength scales with $\sqrt{n}$ due to the operator nature of the coupling term $(\hat{a}^\dagger + \hat{a})$. The Floquet picture, on the other hand, always exhibits the same light-matter coupling strength. This difference between the QED and Floquet pictures has been observed in a recent theoretical study[86].

VI. GENERALIZED HAMILTONIANS FOR MANY MOLECULES AND MODES

The previous sections were chiefly concerned with Hamiltonians under the long-wavelength approximation and for a single photonic mode to more clearly demonstrate the relations between different gauges and representations. However, to accurately reproduce the results of experiments such as those with Fabry–Pérot cavities,[1–7,9,10,12,87–98] these approximations are no longer adequate. In this manner, we must use generalized Hamiltonians to model such systems, so building on the formalism introduced in the previous sections, we use this section as a practical example of creating Hamiltonians that represent more complex systems. In doing so, many modes coupled to many molecules are considered, and we partially relax the long-wavelength approximation such that $\hat{\mathbf{A}}$ is no longer spatially invariant while the matter interactions are still approximated as dipoles. Such a Hamiltonian is necessary to describe many molecules coupled to a Fabry–Pérot cavity, as depicted in Fig. 8a. In that situation, we explicitly consider a 1-D array of molecules.[99] Several useful review articles related to this topic can be found in Ref. 100.

In Fabry–Pérot cavities, the total wavevector of the photon can be decomposed into a component that is perpendicular to the cavity mirror, which we denote as k_z

$$k_z = \frac{n_z \pi}{L_z}, \qquad n_z = 1, 2, ...\infty. \tag{65}$$

The value of k_z is explicitly quantized, due to the boundary condition imposed by two mirrors, where L_z is the distance between the two mirrors. In the literature,[87,88] k_z is often denoted as $k_\perp$ because it is perpendicular to both mirrors (not to be confused with the transverse component of the field in Eq. B3a). There are two more degenerate wavevectors, k_x and k_y, with their directions parallel to the mirror, and are commonly denoted as $k_\parallel$ in the literature (not to be confused with the longitudinal component of the field, such as Eq. B2). Both k_x and k_y are in principle, quasi-continuous because the boundary length for the lateral directions (x and y in Fig. 8) are generally much larger than the mirror distance L_z. The cavity quantization volume is $\mathcal{V} = \mathcal{S} \cdot L_z$, where $\mathcal{S}$ represents the effective quantization area at which molecules are coupled to the cavity. Using the experimentally measured Ω_R and $\mathcal{V}$, one can estimate how many molecules N are effectively coupled to the cavity.[87]

Overall, this leads to many photonic modes that

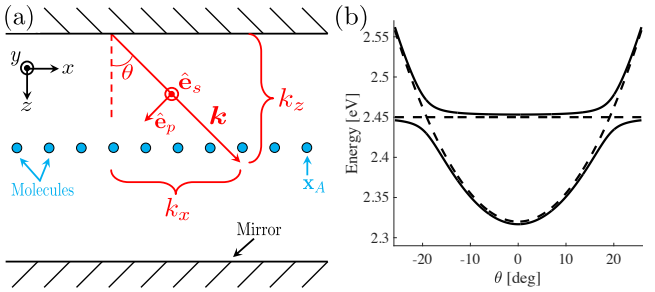

FIG. 8. (a) Schematic of many colinear molecules in a Fabry–Pérot (FP) cavity. $\hat{\mathbf{e}}_s$ and $\hat{\mathbf{e}}_p$ are the unit vectors indicating the directions of the s and p polarized components of $\hat{E}_\perp$, respectively. (b) Schematic dispersion plot of the upper and lower polariton states in a FP cavity (solid lines) as a function of angle (θ) with the same physical parameters as are used in Ref. 87. The dispersion plot of a completely uncoupled system (dashed lines) is also shown to illustrate the Rabi splitting.

can be energetically close to a matter state transition, such as electronic excitations[87,99–105] or vibrational excitations.[2,4,10,91,98,106,107] For these cavities, the photonic dispersion relations are the same for both the transverse electric (TE) and transverse magnetic (TM) polarizations, and experimentally, one can easily access both[105,108,109].

For simplicity, let us focus on the TE mode, and set $k_y = 0$. For a field propagation direction $\mathbf{k}$ (see Fig.8), the total energy of the photon is

$$E_{\rm ph}(\theta) = \hbar\omega_{\boldsymbol{k}} = \frac{\hbar c}{n_{\rm eff}}\sqrt{k_z^2 + k_x^2} = \frac{\hbar c}{n_{\rm eff}} k_z \sqrt{1 + \tan^2\theta}, \tag{66}$$

where c is the speed of the light, $n_{\rm eff}$ is the effective refractive index inside the cavity, and θ is the angle of $\boldsymbol{k}$ from the normal of the mirror (see Fig. 8a). This angle θ is often referred to as the "incident angle" of the photon, which is $\tan\theta = k_x/k_z$. When $\theta = 0$, we have

$$E_{\rm ph}(0) = \frac{\hbar c}{n_{\rm eff}} k_z \equiv \hbar\omega_{\rm c}, \tag{67}$$

where $\omega_{\rm c}$ is the photon frequency of the quantized direction (z-direction) in the cavity, used in the single mode approximation of the cavity QED. Further, under the single mode approximation (by setting $k_x = 0$) the photonic momentum $\mathbf{k}$ (or the field propagation direction) will be perpendicular to the cavity mirror.

In principle, the Fabry–Pérot cavity has an infinite set of possible k_z that satisfy the mirror boundary conditions (Eq. 65). Often, one only considers the k_z that is close to the matter excitation energy. However, when $E_{\rm ph}$ is much smaller than the matter excitation energy, multiple modes that contain various k_z (Eq. 65) in the range of matter-energy and a given range of θ have to be considered.[101,104] In this review, we only consider the case for a single k_z (such that $k_z = \pi/L_z$).

Note that for Fabry–Pérot cavities, $\omega_{\rm k}$ is polarization

independent, so typically only the TM mode is considered. We emphasize that for a *plasmonic* cavity, Eq. 66 no longer always holds. For example, the plasmonic cavity[110,111] has a similar dispersion for the TM polarization $\omega_{\boldsymbol{k},\mathrm{TM}} = \frac{c}{n_{\mathrm{eff}}}\sqrt{k_x^2 + (\frac{2\pi}{a_x})^2}$, but a linear dispersion for the TE mode $\omega_{\boldsymbol{k},\mathrm{TE}} = \frac{c}{n_{\mathrm{eff}}}(\frac{2\pi}{a_x} \pm k_x)$, where a_x is the lattice constant in the x-direction for the plasmonic lattice and n_{eff} is the effective index of refraction of the ambient material in the cavity. Due to this dependence on polarization for the cavity dispersion with plasmonic cavities, both polarizations must be considered for such systems.[110–115] However, for this section, we will focus on Fabry–Pérot cavities. We refer the reader to Ref. 112 for further discussions on plasmonic cavities.

With the motivation of this model in mind, in this section, we present first a generalized dipole-gauge Hamiltonian and then a more approximated generalized Tavis-Cummings Hamiltonian.

A. Generalized Dipole-Gauge Hamiltonian

When considering cavities with many k_x modes, the energy eigenspectrum is typically visualized on a dispersion plot, where the eigenenergies are plotted as a function of k_x. To find these k_x-resolved energies and states, the Hamiltonian in question needs to be truncated to the set of modes with a given k_x. This truncation is classified by the projection operator,

$$\hat{\mathcal{P}}_{k_x} = \hat{\mathbb{1}}_{\mathrm{M}} \otimes \sum_{k_y, n_{k_x,k_z}} \left|n_{k_x,k_z}\right\rangle\!\!\left\langle n_{k_x,k_z}\right|, \tag{68}$$

where $\hat{\mathbb{1}}_{\mathrm{M}}$ is the identity for all matter degrees of freedom, and $\{\left|n_{k_x,k_z}\right\rangle\}$ are the Fock states for a given k_x and k_z. To avoid gauge ambiguities, this mode truncation can be performed as discussed in Ref. 75, where the $\hat{\mathcal{P}}_{k_x}$ enters into the exponential of the PZW operator (See Eq. 41). Then, for each k_x, this truncated Hamiltonian is diagonalized to find the dispersion plots and corresponding Hopfield[116] coefficients as a function of k_x.

To derive such a Hamiltonian, we start from the Minimal Coupling Hamiltonian (Eq. 4), following the framework discussed in Ref. 117. It is convenient to rewrite this Hamiltonian by grouping the matter particles into well-separated molecules, where the intermolecular distances are much longer than the intramolecular distances.

In such circumstances, we can write $\hat{A}(\hat{\mathbf{x}}_j) \approx \hat{A}(\bar{\mathbf{x}}_A)$ for all particles, j, within the molecule, A, with the center of mass, $\bar{\mathbf{x}}_A$. This is a much less restrictive form of the long-wavelength approximation, where now we are just approximating that the field is slowly varying across a given molecule, not the entire system. The total Hamiltonian is then written as

$$\begin{aligned}\hat{H}^{[N]}_{\mathrm{p\cdot A}} = &\sum_{\boldsymbol{k}} \hbar\omega_{\boldsymbol{k}}\hat{a}^\dagger_{\boldsymbol{k}}\hat{a}_{\boldsymbol{k}} + \sum_{A,j\in A}\frac{1}{2m_j}(\hat{\boldsymbol{p}}_j - z_j\hat{\boldsymbol{A}}(\bar{\mathbf{x}}_A))^2 \\ &+ \hat{V}^{AA}_{\mathrm{coul}} + \sum_{A\neq B}\hat{V}^{AB}_{\mathrm{coul}},\end{aligned} \tag{69}$$

where $\{A, B\}$ index over the molecules in the system whose centers of mass are located at $\bar{\mathbf{x}}_A$, $\{j\}$ indexes over each charged particle j in the molecule A, $\hat{V}^{AA}_{\mathrm{coul}}$ is the intramolecular Coulomb potential in molecule A, and $\hat{V}^{AB}_{\mathrm{coul}}$ is the intermolecular Coulomb potential between molecules A and B.

Now to transform this into the dipole gauge, we use the PZW operator (Eq. 5), but now with $\hat{\boldsymbol{A}}(\bar{\mathbf{x}}_A)$ spatially varying inside the cavity (but still approximated as constant within a given molecule):

$$\hat{\boldsymbol{A}}(\bar{\mathbf{x}}_A) = \sum_{\boldsymbol{k},n}\sqrt{\frac{\hbar}{2\epsilon_0\omega_{\boldsymbol{k}}\mathcal{V}}}\hat{\boldsymbol{e}}_n\left[e^{-i\boldsymbol{k}\cdot\bar{\mathbf{x}}_A}\hat{a}^\dagger_{\boldsymbol{k},n} + e^{i\boldsymbol{k}\cdot\bar{\mathbf{x}}_A}\hat{a}_{\boldsymbol{k},n}\right] \tag{70}$$

where the general expression of the quantized electric field $E_\perp$ and magnetic field $\hat{B}$ can be found in standard QED textbooks (for example Refs. 41 and 117 or the Appendix of Ref. 19) or in Appendix B.

The corresponding PZW gauge transform operator becomes a *multi-centered* PZW operator[117,118] expressed as

$$\hat{U}_N = \exp\big[-\frac{i}{\hbar}\sum_{A=1}^{N}\hat{\boldsymbol{\mu}}_A\cdot\hat{\boldsymbol{A}}(\bar{\mathbf{x}}_A)\big], \tag{71}$$

which has specific centers of molecules $\bar{\mathbf{x}}_A$. This $\hat{U}_N$ is still a boost operator on $\hat{\boldsymbol{p}}_j$, since we are still assuming that the individual molecules can be well described by their dipoles, so $\hat{U}_N\hat{\boldsymbol{p}}_j\hat{U}^\dagger_N \approx \hat{\boldsymbol{p}}_j + q_j\hat{\boldsymbol{A}}(\bar{\mathbf{x}}_A)$. We can also evaluate $\hat{U}_N\hat{a}_{\boldsymbol{k}}\hat{U}^\dagger_N$ as,

$$\hat{U}_N\hat{a}_{\boldsymbol{k}}\hat{U}^\dagger_N = \hat{a}_{\boldsymbol{k}} + \sum_A i\sqrt{\frac{\hbar}{2\epsilon_0\omega_{\boldsymbol{k}}\mathcal{V}}}\hat{\boldsymbol{e}}_n\hat{\boldsymbol{\mu}}_A(\hat{\boldsymbol{R}}_A)e^{-i\boldsymbol{k}\cdot\hat{\boldsymbol{x}}_A}, \tag{72}$$

where $\hat{\boldsymbol{\mu}}_A(\hat{\boldsymbol{R}}_A)$ is the dipole operator of molecule A with the nuclear configuration $\hat{\boldsymbol{R}}_A$.

Additionally, the phase rotation from Eq. 9 can be generalized for many modes as

$$\hat{U}^{[N]}_\phi = e^{-i\frac{\pi}{2}\sum_{\mathbf{k},n}\hat{a}^\dagger_{\mathbf{k},n}\hat{a}_{\mathbf{k},n}}, \tag{73}$$

where all the modes now experience a phase rotation.

Now, we can write our generalized dipole gauge Hamil-

tonian in full space as,

$$\hat{H}^{[N]}_{\mathrm{d\cdot E}} = \hat{U}^{[N]}_{\phi}\hat{U}_N\hat{H}^{[N]}_{\mathrm{p\cdot A}}\hat{U}^{\dagger}_N\hat{U}^{[N]\dagger}_{\phi} \tag{74}$$
$$= \hat{H}_{\mathrm{M}} + \sum_{\boldsymbol{k},n}\Bigg[\hbar\omega_{\boldsymbol{k}}(\hat{a}^{\dagger}_{\boldsymbol{k}}\hat{a}_{\boldsymbol{k}} + \frac{1}{2})$$
$$+ \sum_A\Big(\sqrt{\frac{\omega_{\mathbf{k}}}{2}}\boldsymbol{\lambda}_{\boldsymbol{k},n}\cdot\hat{\boldsymbol{\mu}}_A(\mathbf{R}_A)(\hat{a}_{\boldsymbol{k}}e^{i\boldsymbol{k}\cdot\mathbf{x}_A} + \hat{a}^{\dagger}_{\boldsymbol{k}}e^{-i\boldsymbol{k}\cdot\mathbf{x}_A})$$
$$+ \sum_B\frac{1}{2}(\boldsymbol{\lambda}_{\boldsymbol{k},n}\cdot\hat{\boldsymbol{\mu}}_A(\mathbf{R}_A))(\boldsymbol{\lambda}_{\boldsymbol{k},n}\cdot\hat{\boldsymbol{\mu}}_B(\mathbf{R}_B))e^{-i\boldsymbol{k}\cdot(\mathbf{x}_A-\mathbf{x}_B)}\Big)\Bigg],$$

where we introduced a coupling parameter for this more complicated system, $\boldsymbol{\lambda}_{\boldsymbol{k},n} = \sqrt{\frac{1}{\epsilon_0\mathcal{V}}}\hat{\boldsymbol{e}}_{\boldsymbol{k},n}$. While this is rigorous, its computational cost can quickly become enormous. This can be seen by a simple basis size analysis. For j molecules with l states and m modes with n Fock states, the basis size scales as $l^j n^m$. Due to this unfavorable exponential scaling, the generalized Tavis-Cummings Hamiltonian is a useful approximation to simulate these systems.

B. Generalized Tavis-Cummings Hamiltonian

Intuitively, the generalized Tavis-Cummings (GTC) Hamiltonian is to the generalized dipole gauge Hamiltonian as the Jaynes-Cummings Hamiltonian is to the traditional dipole gauge Hamiltonian. In this manner, there are a series of approximations from Eq. 74 to obtain the GTC Hamiltonian. Namely, we first truncate each molecule to the two-level approximation and remove permanent dipole, such that the dipole operator for a given molecule can be written as $\hat{\boldsymbol{\mu}}_A = \boldsymbol{\mu}^{\mathrm{eg}}_A\hat{\sigma}_x$, where $\boldsymbol{\mu}^{\mathrm{eg}}_A$ is the transition dipole moment between the ground and excited states for the molecule A. Then, the dipole self-energy terms (last line of Eq. 74) are entirely neglected. Finally, the rotating wave approximation is performed such that for the interaction terms become:

$$\sqrt{\frac{\omega_{\mathbf{k}}}{2}}\boldsymbol{\lambda}_{\boldsymbol{k},n}\cdot\hat{\boldsymbol{\mu}}_A(\mathbf{R}_A)(\hat{a}_{\boldsymbol{k}}e^{i\boldsymbol{k}\cdot\mathbf{x}_A} + \hat{a}^{\dagger}_{\boldsymbol{k}}e^{-i\boldsymbol{k}\cdot\mathbf{x}_A}) \rightarrow \tag{75}$$
$$\sqrt{\frac{\omega_{\mathbf{k}}}{2}}\boldsymbol{\lambda}_{\boldsymbol{k},n}\cdot\boldsymbol{\mu}^{\mathrm{eg}}_A(\mathbf{R}_A)(\hat{\sigma}^{\dagger}_A\hat{a}_{\boldsymbol{k}}e^{i\boldsymbol{k}\cdot\mathbf{x}_A} + \hat{\sigma}_A\hat{a}^{\dagger}_{\boldsymbol{k}}e^{-i\boldsymbol{k}\cdot\mathbf{x}_A}),$$

where $\hat{\sigma}_A$ is the lowering operator for molecule A's two level system. This series then leads to an expression of the GTC Hamiltonian,

$$\hat{H}_{\mathrm{GTC}} = \hat{H}_{\mathrm{M}} + \sum_{\boldsymbol{k},n}\Bigg[\hbar\omega_{\boldsymbol{k}}(\hat{a}^{\dagger}_{\boldsymbol{k}}\hat{a}_{\boldsymbol{k}} + \frac{1}{2}) \tag{76}$$
$$+ \sqrt{\frac{\omega_{\mathbf{k}}}{2}}\boldsymbol{\lambda}_{\boldsymbol{k},n}\cdot\boldsymbol{\mu}^{\mathrm{eg}}_A(\hat{\sigma}^{\dagger}_A\hat{a}_{\boldsymbol{k}}e^{i\boldsymbol{k}\cdot\mathbf{x}_A} + \hat{\sigma}_A\hat{a}^{\dagger}_{\boldsymbol{k}}e^{-i\boldsymbol{k}\cdot\mathbf{x}_A})\Bigg]$$

The benefit of having this generalized Tavis-Cummings model is that now it is trivial to run simulations in the single excited subspace since different excitation levels are now decoupled from each other. This drastically reduces the computational cost of modeling large systems. Recently, studies involving this GTC Hamiltonian have been able to shine new light on the experimentally found dispersion plots[87,88,119,120] (see Fig. 8(b)).

One such observed phenomenon that can be predicted by the GTC is the presence of collective "bright" and "dark" states formed by the hybridization of each molecule with each k_x mode. Note that these terms refer to the presence (or lack thereof) of photonic character in the energy eigenstates of this system. By hybridizing N singly excited molecular states with 0 photons with a collective molecular ground state with a single photon, $N+1$ energy eigenstates are formed. The upper and lower polaritons make up the two bright states, and the other $N-1$ states become dark states with no photonic character, making them energetically degenerate (see flat dashed line in Fig. 8(b)).

VII. CONCLUSIONS AND OUTLOOK

There has been a great deal of progress in the last few years in understanding different representations and gauges to model these cQED systems. In an effort to summarize the many different approaches to this problem in one place, this review focuses on the various ways to formulate cQED Hamiltonians for different levels of approximation and applications.

Section II discusses three different representations to express the cavity-matter hybrid system in full space. It begins with the minimal coupling Hamiltonian in the Coulomb gauge (Sect. II A), where the light-matter interaction is mediated through the matter momentum and the photonic field's vector potential. Then, the Power-Zienau-Woolly (PZW) transformation is introduced under the long-wavelength approximation (or equivalently dipole approximation), and the dipole gauge and Pauli-Fierz Hamiltonians (Sect. II B) are derived from the minimal coupling Hamiltonian. Finally, a new representation, called the Asymptotically Decoupled Hamiltonian, is presented from the minimal coupling Hamiltonian and its advantageous convergence properties are discussed (Sect. II C).

In Section III, we go on to discuss complications that ensue due to a finite truncation of the infinite Hilbert space Hamiltonians in Section II and their corresponding resolutions. When projecting the dipole gauge Hamiltonian (Sect. II B) and minimal coupling Hamiltonian (Sect. II A) to a finite matter eigenbasis, the polariton energies do not match, indicating that performing a simple projection breaks the gauge invariance (Sect. III A). These gauge ambiguities can be understood since projecting the PZW operator looses its unitary property. By properly truncating all operators, these ambiguities can be resolved a so-called properly truncated Coulomb gauge Hamiltonian is formed (Sect. III B). Building off of this, by performing a change of basis and a phase

rotation, the polarized Fock state representation can be formed from this properly truncated Coulomb gauge Hamiltonian, which for molecular systems can have its eigenspectrum converge for a very small basis set (Sect. III C). It has also been shown that truncating the number of photonic modes also leads to gauge ambiguities that can be resolved using a method similar to the resolution for the matter DOFs (Sect. III D). Additionally, these gauge ambiguities have recently been resolved for Hamiltonians beyond the long-wavelength approximation (Sect. III E).

Section IV then connects the rigorous cQED Hamiltonians from Sections II and III to the more commonly used quantum optic models such as the Jaynes-Cummings model and the Rabi model. This section, carefully discusses the different levels of approximations that each model are under and compares the accuracy of each model.

Additionally, Section V contrasts the cQED methods discussed in this review with the commonly used Floquet theory for laser driven media. This shows the limits in which the cQED methods approach the Floquet picture, as well as the reasons to use one method over another.

Since many experiments are done in Fabry–Pérot cavities, Section VI discusses the Hamiltonians used for such systems. Since Fabry–Pérot cavities are made of flat mirrors, they have a quasi-continuous spectrum of photonic modes and typically hold many molecules, so it is helpful to use Hamiltonians that explicitly consider this. This section discusses the generalized multi-center dipole gauge Hamiltonian that considers many molecules as individual dipoles inside a cavity (Sect. VI A). Then, by making a series of approximations, the generalized Tavis-Cummings Hamiltonian is formulated, which can drastically reduce the computational cost of modeling these very complex systems (Sect. VI B).

Even with the numerous recent advances in the field, there are still many mysteries to be solved in polariton chemistry. Typically, the first step in approaching these challenges is to formulate the Hamiltonian to describe the system. With a summary of the different representations, truncation schemes, and levels of approximation in various cQED Hamiltonians, we hope that this review will provide theorists with a full toolbox such that they can fit the best method to their own application and start unraveling the mysteries of the field.

CONFLICT OF INTEREST

The authors have no conflicts to disclose.

DATA AVAILABILITY

The data that support the findings of this work are available from the corresponding author under reasonable request.

ACKNOWLEDGMENTS

This work was supported by the Air Force Office of Scientific Research under Grant No. FA9550-23-1-0438, as well as by the National Science Foundation Award under Grant No. CHE-2244683. M.T. appreciates the support from the National Science Foundation Graduate Research Fellowship Program under Grant No. DGE-1939268. P. H. appreciates the support of the Cottrell Scholar Award (a program by the Research Corporation for Science Advancement). Computing resources were provided by the Center for Integrated Research Computing (CIRC) at the University of Rochester. The authors want to acknowledge enlightening discussions with Angel Rubio, Abraham Nitzan, Neepa Maitra, Adam Stokes, Ahsan Nazir, Peter Milonni, Sarada Rajeev, Tao Li, Michael Ruggenthaler, and David Reichman.

Appendix A: Review of Molecular Hamiltonians

Here, we briefly review some basic knowledge of the molecular Hamiltonian, which will be useful for our discussions of molecular cavity QED. We begin by defining the matter Hamiltonian as follows

$$\hat{H}_{\mathrm{M}} = \hat{\mathbf{T}} + \hat{V}(\hat{\mathbf{x}}) = \sum_j \frac{1}{2m_j}\hat{\mathbf{p}}_j^2 + \hat{V}(\hat{\mathbf{x}}_j), \tag{A1}$$

where j is the index of the j_{th} charged particle (including all electrons and nuclei), with the corresponding mass, m_j, and *canonical* momentum, $\hat{\mathbf{p}}_j = -i\hbar\boldsymbol{\nabla}_j$. We denote electronic coordinate with $\hat{\mathbf{r}}$, and nuclear coordinate with $\hat{\mathbf{R}}$, and use $\hat{\mathbf{x}}_j \in \{\mathbf{r}_j, \mathbf{R}_j\}$ to represent either the electron or nucleus, with $\hat{\mathbf{x}}$ being the coordinate operator for all charged particles. Further, $\hat{\mathbf{T}} = \hat{\mathbf{T}}_{\mathbf{R}} + \hat{\mathbf{T}}_{\mathbf{r}}$ is the kinetic energy operator for all charged particles, where $\hat{\mathbf{T}}_{\mathbf{R}}$ and $\hat{\mathbf{T}}_{\mathbf{r}}$ represent the kinetic energy operator for nuclei and for electrons, respectively. Further, $\hat{V}(\hat{\mathbf{x}})$ is the potential operator that describes the Coulombic interactions among the electrons and nuclei. The electronic Hamiltonian is often defined as

$$\hat{H}_{\mathrm{el}} = \hat{H}_{\mathrm{M}} - \hat{\mathbf{T}}_{\mathbf{R}} = \hat{\mathbf{T}}_r + \hat{V}(\hat{\mathbf{x}}), \tag{A2}$$

which includes the kinetic energy of electrons, electron-electron interactions, electron-nuclear interactions, and nuclear-nuclear interactions. The essential task of the electronic structure community is focused on solving the eigenstates of $\hat{H}_{\mathrm{el}}$ at a particular nuclear configuration $\mathbf{R}$ as follows

$$\hat{H}_{\mathrm{el}}|\psi_\alpha(\mathbf{R})\rangle = E_\alpha(\mathbf{R})|\psi_\alpha(\mathbf{R})\rangle, \tag{A3}$$

where $E_\alpha(\mathbf{R})$ is commonly referred to as the α_{th} potential energy surface (PES) or adiabatic energy, and $|\psi_\alpha(\mathbf{R})\rangle$ is commonly referred to as the α_{th} adiabatic electronic state.

In the adiabatic electronic basis $\{|\psi_\alpha(\mathbf{R})\rangle\}$, the matter Hamiltonian can be expressed as[66,68]

$$\hat{H}_{\mathrm{M}} = \frac{1}{2\mathbf{M}}\big(\hat{\mathbf{P}} - i\hbar\sum_{\alpha\beta}\mathbf{d}_{\alpha\beta}|\psi_\alpha\rangle\langle\psi_\beta|\big)^2 + \sum_\alpha E_\alpha(\mathbf{R})|\psi_\alpha\rangle\langle\psi_\alpha|, \tag{A4}$$

where $\hat{\mathbf{P}}$ is the nuclear momentum operator, $\mathbf{M}$ is the tensor of nuclear masses, and we have used the shorthand notation $|\psi_\alpha\rangle \equiv |\psi_\alpha(\mathbf{R})\rangle$, and $\mathbf{d}_{\alpha\beta}$ is the derivative coupling expressed as

$$\mathbf{d}_\alpha = \langle\psi_\alpha(\mathbf{R})|\nabla_{\mathbf{R}}|\psi_\alpha(\mathbf{R})\rangle. \tag{A5}$$

Note that the above equation is equivalent[66,68] to the commonly used form of the vibronic Hamiltonian

$$\hat{H}_{\mathrm{M}} = -\frac{\hbar^2}{2\mathbf{M}}\sum_{\alpha\beta}\left[\nabla^2_{\mathbf{R}}\delta_{\alpha\beta} + 2\mathbf{d}_{\alpha\beta}\cdot\nabla_{\mathbf{R}} + D_{\alpha\beta}\right]|\psi_\alpha\rangle\langle\psi_\beta| + \sum_\alpha E_\alpha(\mathbf{R})|\psi_\alpha\rangle\langle\psi_\alpha|,$$

where $D_{\alpha\beta} = \langle\psi_\alpha(\mathbf{R})|\nabla^2_R|\psi_\beta(\mathbf{R})\rangle$ is the second derivative coupling. A simple proof can be found in Ref. 18.

Later, we will see that the dipole operator plays an important role in describing light-matter interactions, so let us spend a bit of time to discuss the molecular dipole operator. The total dipole operator of the entire molecule is

$$\hat{\boldsymbol{\mu}} = \sum_j z_j\hat{\mathbf{x}}_j, \tag{A6}$$

where z_j is the charge for the j_{th} charged particle. The matrix elements of the total dipole operators can be obtained using the adiabatic states as

$$\boldsymbol{\mu}_{\alpha\beta}(\mathbf{R}) = \langle\psi_\alpha(\mathbf{R})|\hat{\boldsymbol{\mu}}|\psi_\beta(\mathbf{R})\rangle. \tag{A7}$$

For $\alpha \neq \beta$, $\boldsymbol{\mu}_{\alpha\beta}(\mathbf{R})$ is referred to as the transition dipole between state $|\psi_\alpha\rangle$ and $|\psi_\beta\rangle$, while $\boldsymbol{\mu}_{\alpha\alpha}(\mathbf{R})$ is commonly referred to as the permanent dipole for state $|\psi_\alpha\rangle$.

It is often difficult to get accurate electronic states for highly excited adiabatic states. It is thus ideal to consider a Hilbert subspace of the electronic Hamiltonian. Considering a finite subset of electronic states $\{|\psi_\alpha\rangle\}$ (see Eq. A3) where there is a total of $\mathcal{N}$ matter states, one can define the following projection operator

$$\hat{\mathcal{P}} = \sum_{\alpha=1}^{\mathcal{N}}|\psi_\alpha(\mathbf{R})\rangle\langle\psi_\alpha(\mathbf{R})|, \tag{A8}$$

which defines the truncation of the full electronic Hilbert space $\hat{\mathbb{1}}_{\mathrm{r}} = \hat{\mathcal{P}} + \hat{\mathcal{Q}}$ which has an infinite basis, to a subspace $\hat{\mathcal{P}}$ that contains a total of $\mathcal{N}$ states, where $\hat{\mathbb{1}}_{\mathrm{r}}$ is the identity operator in the electronic Hilbert subspace (the subspace containing all of the electron DOF) and $\hat{\mathcal{Q}} = \hat{\mathbb{1}}_{\mathrm{r}} - \hat{\mathcal{P}}$ is the subspace being projected out.

Using the projection operator, one can define the projected matter Hamiltonian (or the truncated matter Hamiltonian) as follows

$$\hat{\mathcal{H}}_{\mathrm{M}} = \hat{\mathcal{P}}\hat{H}_{\mathrm{M}}\hat{\mathcal{P}} = \hat{\mathcal{P}}\hat{\mathbf{T}}\hat{\mathcal{P}} + \hat{\mathcal{P}}\hat{V}(\hat{\mathbf{x}})\hat{\mathcal{P}}. \tag{A9}$$

Throughout this review, we use calligraphic symbols (such as $\hat{\mathcal{H}}_{\mathrm{M}}$) to indicate operators in the truncated Hilbert space.

One can also explicitly write the dipole operator in the truncated Hilbert space as follows

$$\hat{\mathcal{P}}\hat{\boldsymbol{\mu}}\hat{\mathcal{P}} = \sum_{\alpha=1}^{\mathcal{N}}\boldsymbol{\mu}_{\alpha\alpha}(\mathbf{R})\ |\psi_\alpha(\mathbf{R})\rangle\langle\psi_\alpha(\mathbf{R})| + \sum_{\alpha\neq\beta}\boldsymbol{\mu}_{\alpha\beta}(\mathbf{R})\ |\psi_\alpha(\mathbf{R})\rangle\langle\psi_\beta(\mathbf{R})|. \tag{A10}$$

In the *same* truncated electronic subspace as defined by $\hat{\mathcal{P}}$ (Eq. A8), we can diagonalize the dipole matrix in Eq. A10 to obtain

$$\hat{\mathcal{P}}\hat{\boldsymbol{\mu}}\hat{\mathcal{P}} = \sum_\nu^{\mathcal{N}}\boldsymbol{\mu}_{\nu\nu}(\mathbf{R})\ |\phi_\nu\rangle\langle\phi_\nu|, \tag{A11}$$

where $|\phi_\nu\rangle$ is the eigenstate of the projected dipole operator $\hat{\mathcal{P}}\hat{\boldsymbol{\mu}}\hat{\mathcal{P}}$ with

$$|\phi_\nu\rangle = \sum_\alpha^{\mathcal{N}} c_\alpha^\nu(\mathbf{R})|\psi_\alpha(\mathbf{R})\rangle, \tag{A12}$$

and $c_\alpha^\nu(\mathbf{R}) = \langle\psi_\alpha(\mathbf{R})|\phi_\nu\rangle$.

The projection operator in Eq. A8 can also be expressed as

$$\hat{\mathcal{P}} = \sum_{\nu=1}^{\mathcal{N}}|\phi_\nu\rangle\langle\phi_\nu|, \tag{A13}$$

which is simply a unitary transform of Eq. A8 (from the $|\psi_\alpha(\mathbf{R})\rangle$-representation to the $|\phi_\nu\rangle$-representation).

In the literature, the eigenstates of $\hat{\mathcal{P}}\hat{\boldsymbol{\mu}}\hat{\mathcal{P}}$, $\{|\phi_\nu\rangle\}$, are referred to as the Mulliken-Hush (MH) diabatic states[64,69,121–123], which are commonly used as approximate *diabatic* states that are defined based on their characters. They are approximate diabatic states in the sense that

$$\langle\phi_\nu|\nabla_{\mathbf{R}}|\phi_\epsilon\rangle \approx 0; \tag{A14}$$

hence, we drop the $\mathbf{R}$-dependence in $|\phi_\nu\rangle$. Constructing rigorous diabatic states (where the derivative coupling is rigorously zero for all possible nuclear configurations) in a finite set of electronic Hilbert spaces is generally impossible, except for diatomic molecules. Recent theoretical progress on diabatization can be found in Ref.[67,124,125].

In the electronic subspace defined within the MH diabatic subspace using $\hat{\mathcal{P}}$ (Eq. A13), $\hat{H}_{\mathrm{el}}$ (Eq. A2) has off-diagonal (or "diabatic") coupling terms

$$V_{\nu\epsilon}(\mathbf{R}) = \langle\phi_\nu|\hat{H}_{\mathrm{el}}|\phi_\epsilon\rangle = \sum_\alpha c_\alpha^{\nu*}(\mathbf{R})c_\alpha^\epsilon(\mathbf{R})\,\langle\psi_\alpha|\,\hat{H}_{\mathrm{el}}\,|\psi_\alpha\rangle \tag{A15}$$

We can explicitly express the matter state projected

$$\hat{\mathcal{H}}_{\mathrm{M}} = \hat{T}_{\mathbf{R}} + \sum_{\nu} V_{\nu\nu}(\mathbf{R})\ |\psi_\nu\rangle\langle\psi_\nu| + \sum_{\nu\neq\epsilon} V_{\nu\epsilon}(\mathbf{R})\ |\psi_\nu\rangle\langle\psi_\epsilon|. \tag{A16}$$

This is also the molecular Hamiltonian for any diabatic representation.

Appendix B: Review of Quantum Electrodynamics

We provide a quick review of quantum electrodynamics (QED).[17,21] We begin by writing the electric field as $\hat{\mathbf{E}}(\mathbf{r}) = \hat{\mathbf{E}}_{\parallel}(\mathbf{r}) + \hat{\mathbf{E}}_{\perp}(\mathbf{r})$, with its longitudinal part $\hat{\mathbf{E}}_{\parallel}(\mathbf{r})$ that is curl-free (irrotational), $\nabla \times \hat{\mathbf{E}}_{\parallel}(\mathbf{r}) = 0$, and the transverse part, $\hat{\mathbf{E}}_{\perp}(\mathbf{r})$, that is divergence-free (solenoidal), $\nabla \cdot \hat{\mathbf{E}}_{\perp}(\mathbf{r}) = 0$. The magnetic field is purely transverse $\hat{\mathbf{B}}(\mathbf{r}) = \hat{\mathbf{B}}_{\perp}(\mathbf{r})$, because it is divergence-free $\nabla \cdot \hat{\mathbf{B}}(\mathbf{r}) = 0$. These fields have spatial dependence, with spatial coordinate $\mathbf{r}$ (not to be confused with the electronic coordinate operator, $\hat{\mathbf{r}}$).

In the context of cavity QED, most simulations are performed in one of two gauges, either the Coulomb gauge[41] or the dipole gauge,[126–128] where the term "gauge" refers to the specific representation of the vector potential $\hat{\mathbf{A}}$. Expressing $\hat{\mathbf{A}} = \hat{\mathbf{A}}_{\parallel} + \hat{\mathbf{A}}_{\perp}$, with its longitudinal part $\hat{\mathbf{A}}_{\parallel}$ that is curl-free $\nabla \times \hat{\mathbf{A}}_{\parallel} = 0$, and the transverse part $\hat{\mathbf{A}}_{\perp}$ that is divergence-free $\nabla \cdot \mathbf{A}_{\perp} = 0$. In principle, one can do gauge transformations that change the longitudinal part $\hat{\mathbf{A}}_{\parallel}$, because the physically observed quantities will not change (e.g. the magnetic field, since $\hat{\mathbf{B}} = \nabla \times \hat{\mathbf{A}} = \nabla \times \hat{\mathbf{A}}_{\perp}$). One often refers to fixing a gauge by choosing the value of $\nabla \times \hat{\mathbf{A}}$ such that the gauge transformation is effectively adding an additional $\nabla\chi$ component to $\hat{\mathbf{A}}_{\parallel}$, which is purely longitudinal because when χ is a scalar function in space, $\nabla\chi$ is curl-free ($\nabla \times \nabla\chi = 0$).

When deriving QED from first principles, one often uses the minimal coupling Hamiltonian in the Coulomb gauge[129] (See Eq. 4). From there, the electric-dipole Hamiltonian can be found via a gauge transformation. The commonly used Pauli-Fierz (PF) QED Hamiltonian[17,21,43] (See Eq. 10) in recent studies of polariton chemistry can be obtained by applying another gauge transformation on the electric-dipole Hamiltonian. We will further discuss the consequence of matter state truncation on gauge invariance, the connection with the commonly used quantum optics model Hamiltonians, and when they will break down in molecular QED.

When fixing a specific gauge, one defines the gauge-dependent vector and scalar potentials for the electromagnetic field. By choosing the Coulomb Gauge (i.e. by enforcing $\nabla \cdot \mathbf{A} = 0$) which makes the vector potential purely transverse, $\hat{\mathbf{A}} = \hat{\mathbf{A}}_{\perp}$, the Hamiltonian of point charge particles (including both electrons and nuclei) interacting with the electromagnetic field can be written as follows[41]

$$\begin{aligned}\hat{H} = &\sum_{j}^{N} \frac{1}{2m_j}\big(\hat{\mathbf{p}}_j - q_j\hat{\mathbf{A}}_{\perp}(\mathbf{r}_j)\big)^2 + \frac{\epsilon_0}{2}\int dr^3 \hat{\mathbf{E}}_{\parallel}^2(\mathbf{r}) \\ &+ \frac{\epsilon_0}{2}\int dr^3\big[\hat{\mathbf{E}}_{\perp}^2(\mathbf{r}) + c^2\hat{\mathbf{B}}_{\perp}^2(\mathbf{r})\big],\end{aligned} \tag{B1}$$

where the sum includes *both* the nuclear and electronic DOFs, $\mathbf{r}_j$ and $\mathbf{p}_j$ are the position and momentum of the charged particle j, with the charge q_j and mass m_j. Further, $\mathbf{A}_{\perp}(\mathbf{r})$, $\mathbf{E}_{\perp}(\mathbf{r})$ and $\mathbf{B}_{\perp}(\mathbf{r})$ are the transverse vector potential, electric field, and magnetic field, respectively. The energy associated with $\mathbf{E}_{\parallel}(\mathbf{r})$ (the second term in Eqn. B1) is given by

$$\begin{aligned}&\frac{\epsilon_0}{2}\int dr^3 \hat{\mathbf{E}}_{\parallel}^2(\mathbf{r}) \\ &= \sum_j \frac{q_j^2}{2\epsilon_0(2\pi)^3}\int \frac{dk^3}{k^2} + \frac{1}{8\pi\epsilon_0}\sum_{i\neq j}\frac{q_i q_j}{|\hat{\mathbf{x}}_i - \hat{\mathbf{x}}_j|} \\ &= \sum_j \epsilon_j^{\infty} + \hat{V}(\hat{\mathbf{x}}) \to \hat{V}(\hat{\mathbf{x}}).\end{aligned} \tag{B2}$$

Here, the first term $\sum_j \epsilon_j^{\infty}$ in the third line of Eqn. B2 is a time-independent infinite quantity that is referred to as the self-energy (not to be confused with the dipole self-energy), which can be regarded as a shift of the zero-point energy[130] and is dropped in the last line of the above equation. In short, the Coulomb potential $V_{\mathrm{coul}}(\hat{\mathbf{x}}) \equiv V(\hat{\mathbf{x}})$ emerges from the longitudinal electric field.

The last term in Eqn. B1 is the energy associated with the transverse fields $\hat{\mathbf{E}}_{\perp}(\mathbf{r})$ and $\hat{\mathbf{B}}_{\perp}(\mathbf{r})$. The general expressions for $\hat{\mathbf{A}}_{\perp}(\mathbf{r})$, $\hat{\mathbf{E}}_{\perp}(\mathbf{r})$, and $\hat{\mathbf{B}}_{\perp}(\mathbf{r})$ are[41]

$$\hat{\mathbf{A}}_{\perp}(\mathbf{r}) = \sum_{\mathbf{k}} \frac{\hat{\mathbf{e}}_{\mathbf{k}}}{\omega_{\mathbf{k}}}\sqrt{\frac{\hbar\omega_{\mathbf{k}}}{2\varepsilon_0\mathcal{V}}}\left(\hat{a}_{\mathbf{k}}e^{i\mathbf{k}\cdot\mathbf{r}} + \hat{a}_{\mathbf{k}}^{\dagger}e^{-i\mathbf{k}\cdot\mathbf{r}}\right), \tag{B3a}$$

$$\hat{\mathbf{E}}_{\perp}(\mathbf{r}) = i\sum_{\mathbf{k}} \hat{\mathbf{e}}_{\mathbf{k}}\sqrt{\frac{\hbar\omega_{\mathbf{k}}}{2\varepsilon_0\mathcal{V}}}\left(\hat{a}_{\mathbf{k}}e^{i\mathbf{k}\cdot\mathbf{r}} - \hat{a}_{\mathbf{k}}^{\dagger}e^{-i\mathbf{k}\cdot\mathbf{r}}\right), \tag{B3b}$$

$$\hat{\mathbf{B}}_{\perp}(\mathbf{r}) = i\sum_{\mathbf{k}} \frac{\mathbf{k}\times\hat{\mathbf{e}}_{\mathbf{k}}}{\omega_{\mathbf{k}}}\sqrt{\frac{\hbar\omega_{\mathbf{k}}}{2\varepsilon_0\mathcal{V}}}\left(\hat{a}_{\mathbf{k}}e^{i\mathbf{k}\cdot\mathbf{r}} - \hat{a}_{\mathbf{k}}^{\dagger}e^{-i\mathbf{k}\cdot\mathbf{r}}\right), \tag{B3c}$$

where $\hat{a}_{\mathbf{k}}^{\dagger}$ and $\hat{a}_{\mathbf{k}}$ are the raising and lowering operator of the mode that has a wavevector of $\mathbf{k} \equiv (k_x, k_y, k_z)$, and they satisfy the canonical commutation relation[41]

$$[\hat{a}_{\mathbf{k}}^{\dagger}, \hat{a}_{\mathbf{k}'}] = \delta_{\mathbf{k},\mathbf{k}'} \cdot \hat{\mathbb{1}}_{\mathbf{k}}. \tag{B4}$$

$\hat{a}_{\mathbf{k}}^{\dagger}$ and $\hat{a}_{\mathbf{k}}$ are the creation and annihilation operators of the photon, respectively, $\delta_{\mathbf{k},\mathbf{k}'}$ is the Kronecker delta, and the frequency of mode $\mathbf{k}$ is $\omega_j = c|\mathbf{k}|$. Here $\mathbf{k} = |\mathbf{k}|\hat{\mathbf{k}}$ aligns in the direction of the unit vector $\hat{\mathbf{k}}$ and $\hat{\mathbf{e}}_{\mathbf{k}} \perp \hat{\mathbf{k}}$ is the polarization unit vector for $\hat{\mathbf{E}}_{\perp}(\mathbf{r})$ and $\hat{\mathbf{A}}_{\perp}(\mathbf{r})$. The polarization of the photonic field can be written as a linear combination of the transverse electric (TE) polarization, $\hat{\mathbf{e}}_{\mathbf{k},\mathrm{TE}}$, and the transverse magnetic (TM) polarization, $\hat{\mathbf{e}}_{\mathbf{k},\mathrm{TM}}$, in relation to a given interface and propagation direction. The TE mode's polarization, $\hat{\mathbf{e}}_{\mathbf{k},\mathrm{TE}}$,

is defined as being perpendicular to the propagation direction and parallel to the interface. The TM mode's polarization, $\hat{\mathbf{e}}_{\mathbf{k},\mathrm{TM}}$, is defined as being perpendicular to both the propagation direction and the TE polarization. For a given polarization, $\hat{\mathbf{e}}_{\mathbf{k}}$, the transverse electric field is along $\hat{\mathbf{e}}_{\mathbf{k}}$ and the magnetic field is along the $\hat{\mathbf{k}}\times\hat{\mathbf{e}}_{\mathbf{k}}$ direction. For example, for the TM mode, the transverse electric field polarization is along $\hat{\mathbf{e}}_{\mathbf{k},\mathrm{TE}}$ and the transverse magnetic field polarization is along $-\hat{\mathbf{e}}_{\mathbf{k},\mathrm{TM}}$.

When considering a planar Fabry-Pérot (FP) microcavity, $\hat{\mathbf{A}}_\perp(\mathbf{r})$, $\hat{\mathbf{E}}_\perp(\mathbf{r})$ and $\hat{\mathbf{B}}_\perp(\mathbf{r})$ satisfy the boundary conditions and thus the wavevector $\mathbf{k}$ becomes quantized[41,130]. For cavity mirrors imposing a boundary condition along z direction (see Fig. 8), the z component of the wavevector $k_z = n\frac{\pi}{L_z}$ with $n = 1, 2, 3...$ as a positive integer. Note that k_x and k_y still remain quasi-continuous variables. These are discussed in details in Sect. VI.

Using the above expressions, the energy of the transverse fields, *i.e.*, the last term in Eqn. B1 is quantized as follows

$$\frac{\varepsilon_0}{2}\int_{\mathcal{V}} dr^3[\mathbf{E}_\perp{}^2(\mathbf{r}) + c^2\mathbf{B}_\perp{}^2(\mathbf{r})] = \sum_{\mathbf{k}}\big(\hat{a}^\dagger_{\mathbf{k}}\hat{a}_{\mathbf{k}} + \frac{1}{2}\big)\hbar\omega_{\mathbf{k}}, \tag{B5}$$

where the spatial integral dr^3 is done within the effective quantized volume $\mathcal{V}$ of the cavity. Thus, Eq. B1 is quantized as

$$\hat{H}_{\mathrm{p\cdot A}} = \sum_j^N \frac{1}{2m_j}\Big(\hat{\mathbf{p}}_j - z_j\hat{\mathbf{A}}_\perp(\hat{\mathbf{x}}_j)\Big)^2 + \hat{V}(\hat{\mathbf{x}}) + \sum_{\mathbf{k}}\big(\hat{a}^\dagger_{\mathbf{k}}\hat{a}_{\mathbf{k}} + \frac{1}{2}\big)\hbar\omega_{\mathbf{k}}. \tag{B6}$$

This is commonly referred to as the "$\mathrm{p}\cdot\mathrm{A}$" or the minimal coupling QED Hamiltonian, in the sense that the light and matter coupling is only carried through the matter momentum and the vector potential of the field. The minimal coupling structure in Eq. 4 comes naturally due to the local $U(1)$ symmetry of the EM field, which is an Abelian gauge field.

Assuming that the size of the molecular system is much smaller than the length of the cavity in the quantized direction, which is commonly referred to as the *long-wavelength approximation*, the transverse fields can be treated as spatially uniform, *i.e.*, $e^{i\mathbf{k}\cdot\mathbf{r}} \approx 1$, such that

$$\hat{\mathbf{A}}_\perp(\mathbf{r}) \approx \hat{\mathbf{A}}_\perp = \sum_{\mathbf{k}}\frac{\hat{\mathbf{e}}_{\mathbf{k}}}{\omega_{\mathbf{k}}}\sqrt{\frac{\hbar\omega_{\mathbf{k}}}{2\varepsilon_0\mathcal{V}}}(\hat{a}_{\mathbf{k}} + \hat{a}^\dagger_{\mathbf{k}}). \tag{B7}$$

Appendix C: Derivation of Baker–Campbell–Hausdorff Identity

For the Properly Truncated Coulomb Gauge Hamiltonian (see Sect. III B), the residual momentum, $\tilde{\mathbf{P}}_{\mathbf{j}}$, and the transformed electronic Hamiltonian, $\hat{\mathcal{U}}^\dagger\hat{\mathcal{H}}_{\mathrm{el}}\hat{\mathcal{U}}$, must be found by using the Baker–Campbell–Hausdorff (BCH) Identity, which is of the form,

$$e^{\hat{A}}\hat{B}e^{-\hat{A}} = \hat{B} + [\hat{A},\hat{B}] + \frac{1}{2!}[\hat{A},[\hat{A},\hat{B}]] + \frac{1}{3!}[\hat{A},[\hat{A},[\hat{A},\hat{B}]]] + \cdots, \tag{C1}$$

where $\hat{A}$ and $\hat{B}$ are arbitrary operators.

To derive this identity, we first define a function $\hat{f}(\lambda)$,

$$\hat{f}(\lambda) = e^{\lambda\hat{A}}\hat{B}e^{-\lambda\hat{A}}, \tag{C2}$$

where λ is a scalar parameter. With this formalism, $\hat{f}(0) = \hat{B}$ and $\hat{f}(1) = e^{\hat{A}}\hat{B}e^{-\hat{A}}$. We can then write $f(1)$ by Taylor expanding about $\lambda = 0$,

$$\hat{f}(1) = \hat{B} + \sum_{n=1}^{\infty}\frac{1}{n!}\left.\frac{\mathrm{d}\hat{f}^n(\lambda)}{\mathrm{d}\lambda^n}\right|_{\lambda=0} \tag{C3}$$

By using the commutation relation, $[\hat{A}, \exp(\pm\lambda\hat{A})] = 0$, the first derivative of $\hat{f}(\lambda)$ can be expressed as,

$$\begin{aligned}\frac{\mathrm{d}\hat{f}(\lambda)}{\mathrm{d}\lambda} &= e^{\lambda\hat{A}}\hat{A}\hat{B}e^{-\lambda\hat{A}} + e^{\lambda\hat{A}}\hat{B}(-\hat{A})e^{-\lambda\hat{A}} \\ &= e^{\lambda\hat{A}}[\hat{A},\hat{B}]e^{-\lambda\hat{A}}.\end{aligned} \tag{C4}$$

By recursion the n^{th} derivative becomes apparent. Since the $\hat{B}$ in Eq. C2 is any arbitrary operator, the n^{th} derivative can be expressed in a similar manner to the first derivative,

$$\frac{\mathrm{d}\hat{f}^n(\lambda)}{\mathrm{d}\lambda^n} = e^{\lambda\hat{A}}\left[\hat{A}, \frac{\mathrm{d}\hat{f}^{n-1}(0)}{\mathrm{d}\lambda^{n-1}}\right]e^{-\lambda\hat{A}}. \tag{C5}$$

By evaluating Eq. C5 at $\lambda = 0$ for each n and inputting the values into Eq. C3, we get,

$$\hat{f}(1) = \hat{B} + [\hat{A},\hat{B}] + \frac{1}{2!}[\hat{A},[\hat{A},\hat{B}]] + \frac{1}{3!}[\hat{A},[\hat{A},[\hat{A},\hat{B}]]] + \cdots, \tag{C6}$$

which perfectly agrees with the statement of the BCH identity in Eq. C1.

[1] J. A. Hutchison, T. Schwartz, C. Genet, E. Devaux, and T. W. Ebbesen, Angew. Chem. Int. Ed. **51**, 1592 (2012).
[2] A. Thomas, J. George, A. Shalabney, M. Dryzhakov, S. J. Varma, J. Moran, T. Chervy, X. Zhong, E. Devaux, C. Genet, J. A. Hutchison, and T. W. Ebbesen, Angew. Chem. Int. Ed. **55**, 11462 (2016).
[3] T. W. Ebbesen, Acc. Chem. Res. **49**, 2403 (2016).
[4] A. Thomas, L. Lethuillier-Karl, K. Nagarajan, R. M. A. Vergauwe, J. George, T. Chervy, A. Shalabney, E. Devaux, C. Genet, J. Moran, and T. W. Ebbesen, Science **363**, 615 (2019).
[5] A. Thomas, A. Jayachandran, L. Lethuillier-Karl, R. M. A. Vergauwe, K. Nagarajan, E. Devaux, C. Genet, J. Moran, and T. W. Ebbesen, Nanophotonics **9**, 249 (2020).
[6] A. Sau, K. Nagarajan, B. Patrahau, L. Lethuillier-Karl, R. M. A. Vergauwe, A. Thomas, J. Moran, C. Genet, and T. W. Ebbesen, Angew. Chem. Int. Ed. **60**, 5712 (2021).
[7] J. Lather, P. Bhatt, A. Thomas, T. W. Ebbesen, and J. George, Angew. Chem. Int. Ed. **58**, 10635 (2019).
[8] J. Lather and J. George, J. Phys. Chem. Lett. **12**, 379 (2020).

[9] J. George, T. Chervy, A. Shalabney, E. Devaux, H. Hiura, C. Genet, and T. W. Ebbesen, Phys. Rev. Lett. **117**, 153601 (2016).
[10] R. M. A. Vergauwe, A. Thomas, K. Nagarajan, A. Shalabney, J. George, T. Chervy, M. Seidel, E. Devaux, V. Torbeev, and T. W. Ebbesen, Angew. Chem. Int. Ed. **58**, 15324 (2019).
[11] K. Hirai, J. A. Hutchison, and H. Uji-i, ChemPlusChem **85**, 1981 (2020).
[12] F. J. Garcia-Vidal, C. Ciuti, and T. W. Ebbesen, Science **373** (2021), 10.1126/science.abd0336.
[13] F. Herrera and F. C. Spano, Phys. Rev. Lett. **116**, 238301 (2016).
[14] M. Kowalewski, K. Bennett, and S. Mukamel, J. Chem. Phys. **144**, 054309 (2016).
[15] A. Semenov and A. Nitzan, J. Chem. Phys. **150**, 174122 (2019).
[16] J. Galego, C. Climent, F. J. Garcia-Vidal, and J. Feist, Phys. Rev. X **9**, 021057 (2019).
[17] V. Rokaj, D. M. Welakuh, M. Ruggenthaler, and A. Rubio, J. Phys. B: At. Mol. Opt. Phys. **51**, 034005 (2018).
[18] A. Mandal, S. M. Vega, and P. Huo, J. Phys. Chem. Lett. **11**, 9215 (2020).
[19] A. Mandal, T. D. Krauss, and P. Huo, J. Phys. Chem. B **124**, 6321 (2020).
[20] C. Schäfer, M. Ruggenthaler, V. Rokaj, and A. Rubio, ACS Photonics **7**, 975 (2020).
[21] C. Schäfer, M. Ruggenthaler, and A. Rubio, Phys. Rev. A **98**, 043801 (2018).
[22] M. Ruggenthaler, J. Flick, C. Pellegrini, H. Appel, I. V. Tokatly, and A. Rubio, Phys. Rev. A **90**, 012508 (2014).
[23] J. A. C. Gonzalez-Angulo and J. Yuen-Zhou, J. Chem. Phys. **152**, 161101 (2020).
[24] J. F. Triana, F. J. Hernández, and F. Herrera, J. Chem. Phys. **152**, 234111 (2020).
[25] P. Martinez, B. Rosenzweig, N. M. Hoffmann, L. Lacombe, and N. T. Maitra, J. Chem. Phys. **154**, 014102 (2021).
[26] K. B. Arnardottir, A. J. Moilanen, A. Strashko, P. Törmä, and J. Keeling, Phys. Rev. Lett. **125**, 233603 (2020).
[27] P. Forn-Díaz, L. Lamata, E. Rico, J. Kono, and E. Solano, Rev. Mod. Phys. **91**, 025005 (2019).
[28] A. F. Kockum, A. Miranowicz, S. D. Liberato, S. Savasta, and F. Nori, Nat. Rev. Phys. **1**, 19 (2019).
[29] A. L. Boité, Adv. Quantum Technol. **3**, 1900140 (2020).
[30] S. D. Liberato, Phys. Rev. Lett. **112**, 016401 (2014).
[31] O. D. Stefano, A. Settineri, V. Macrì, L. Garziano, R. Stassi, S. Savasta, and F. Nori, Nat. Phys. **15**, 803 (2019).
[32] D. D. Bernardis, T. Jaako, and P. Rabl, Phys. Rev. A **97**, 043820 (2018).
[33] D. D. Bernardis, P. Pilar, T. Jaako, S. D. Liberato, and P. Rabl, Phys. Rev. A **98**, 053819 (2018).
[34] L. A. Martínez-Martínez, R. F. Ribeiro, J. C. González-Angulo, and J. Yuen-Zhou, ACS Photonics **5**, 167 (2017).
[35] Y. Ashida, A. İmamoğlu, and E. Demler, Phys. Rev. Lett. **126**, 153603 (2021).
[36] M. A. D. Taylor, A. Mandal, W. Zhou, and P. Huo, Phys. Rev. Lett. **125**, 123602 (2020).
[37] A. Stokes and A. Nazir, Nat. Commun. **10** (2019), 10.1038/s41467-018-08101-0.
[38] F. J. Hernández and F. Herrera, J. Chem. Phys. **151**, 144116 (2019).
[39] B. M. Weight, T. D. Krauss, and P. Huo, The Journal of Physical Chemistry Letters **14**, 5901 (2023), pMID: 37343178, https://doi.org/10.1021/acs.jpclett.3c01294.
[40] E. A. Power and S. Zienau, Philos. Trans. Royal Soc. A **251**, 427 (1959).
[41] C. Cohen-Tannoudji, J. Dupont-Roc, and G. Grynberg, *Photons and Atoms: Introduction to Quantum Electrodynamics* (Wiley, 1997).
[42] M. Göppert-Mayer, Ann. Phys. **18**, 466 (2009).
[43] J. Flick, M. Ruggenthaler, H. Appel, and A. Rubio, Proc. Natl. Acad. Sci. **114**, 3026 (2017).
[44] J. Wang, B. Weight, and P. Huo, "Investigating Cavity Quantum Electrodynamics-Enabled Endo/Exo- Selectivities in a diels-alder reaction," (2024), chemRxiv, 10.26434/chemrxiv-2024-6xsr6-v2.
[45] B. M. Weight, X. Li, and Y. Zhang, Phys. Chem. Chem. Phys. **25**, 31554 (2023).
[46] B. M. Weight, S. Tretiak, and Y. Zhang, Phys. Rev. A **109**, 032804 (2024).
[47] B. M. Weight, D. J. Weix, Z. J. Tonzetich, T. D. Krauss, and P. Huo, J. Am. Chem. Soc. (2024), 10.1021/jacs.4c04045.
[48] W. Ying and P. Huo, ChemRxiv (2024), 10.26434/chemrxiv-2024-sl6lt-v2.
[49] W. Ying, M. A. D. Taylor, and P. Huo, Nanophotonics **13**, 2601 (2024).
[50] S. Montillo Vega, W. Ying, and P. Huo, ChemRxiv (2024), 10.26434/chemrxiv-2024-m7t4c.
[51] N. M. Hoffmann, C. Schäfer, N. Säkkinen, A. Rubio, H. Appel, and A. Kelly, J. Chem. Phys. **151**, 244113 (2019).
[52] T. E. Li, H.-T. Chen, A. Nitzan, and J. E. Subotnik, Phys. Rev. A **101**, 033831 (2020).
[53] M. A. D. Taylor, B. M. Weight, and P. Huo, Phys. Rev. B **109**, 104305 (2024).
[54] S. Shin and H. Metiu, J. Chem. Phys. **102**, 9285 (1995).
[55] A. Stokes and A. Nazir, "Gauge non-invariance due to material truncation in ultrastrong-coupling qed," (2020), arxiv:2005.06499.
[56] E. Rousseau and D. Felbacq, Sci. Rep. **7** (2017), 10.1038/s41598-017-11076-5.
[57] A. Stokes and A. Nazir, Rev. Mod. Phys. **94**, 045003 (2022).
[58] M. Roth, F. Hassler, and D. P. DiVincenzo, Phys. Rev. Research **1**, 033128 (2019).
[59] A. Settineri, O. D. Stefano, D. Zueco, S. Hughes, S. Savasta, and F. Nori, Phys. Rev. Research **3**, 023079 (2021).
[60] W. E. Lamb, R. R. Schlicher, and M. O. Scully, Phys. Rev. A **36**, 2763 (1987).
[61] K. Rzazewski and R. W. Boyd, J. Mod. Optic. **51**, 1137 (2004).
[62] L. Garziano, A. Settineri, O. D. Stefano, S. Savasta, and F. Nori, Phys. Rev. A **102**, 023718 (2020).
[63] C. A. Mead and D. G. Truhlar, J. Chem. Phys. **77**, 6090 (1982).
[64] R. J. Cave and M. D. Newton, Chem. Phys. Lett. **249**, 15 (1996).
[65] H. Guo and D. R. Yarkony, Phys. Chem. Chem. Phys. **18**, 26335 (2016).
[66] T. Pacher, C. A. Mead, L. S. Cederbaum, and H. Köppel, J. Chem. Phys. **91**, 7057 (1989).
[67] J. E. Subotnik, E. C. Alguire, Q. Ou, B. R. Landry, and S. Fatehi, Acc. Chem. Res. **48**, 1340 (2015).
[68] G. A. Worth and L. S. Cederbaum, Annu. Rev. Phys. Chem. **55**, 127 (2004).
[69] R. J. Cave and M. D. Newton, J. Chem. Phys. **106**, 9213 (1997).
[70] E. K. Irish, J. Gea-Banacloche, I. Martin, and K. C. Schwab, Phys. Rev. B **72**, 195410 (2005).
[71] E. K. Irish, Phys. Rev. Lett. **99**, 173601 (2007).
[72] S. Schweber, Ann. Phys. (NY) **41**, 205 (1967).
[73] V. V. Albert, G. D. Scholes, and P. Brumer, Phys. Rev. A **84**, 042110 (2011).
[74] S. Agarwal, S. M. H. Rafsanjani, and J. H. Eberly, Phys. Rev. A **85**, 043815 (2012).
[75] M. A. D. Taylor, A. Mandal, and P. Huo, Opt. Lett. **47**, 1446 (2022).
[76] C. Gustin, S. Franke, and S. Hughes, arXiv (2022), 10.48550/ARXIV.2208.11796, arxiv:2208.11796.
[77] E. T. Jaynes and F. W. Cummings, Proc. IEEE **51**, 89 (1963).
[78] B. Mischuck and K. Mølmer, Phys. Rev. A **87**, 022341 (2013).
[79] M. Hofheinz, E. M. Weig, M. Ansmann, R. C. Bialczak, E. Lucero, M. Neeley, A. D. O'Connell, H. Wang, J. M. Martinis, and A. N. Cleland, Nature **454**, 310 (2008).
[80] M. Hofheinz, H. Wang, M. Ansmann, R. C. Bialczak, E. Lucero, M. Neeley, A. D. O'Connell, D. Sank, J. Wenner, J. M. Martinis, and A. N. Cleland, Nature **459**, 546 (2009).
[81] H. Hübener, U. D. Giovannini, C. Schäfer, J. Andberger,

M. Ruggenthaler, J. Faist, and A. Rubio, Nat. Mater. **20**, 438 (2020).
[82]M. Holthaus, J. Phys. B: At. Mol. Opt. Phys. **49**, 013001 (2015).
[83]H. Sambe, Phys. Rev. A **7**, 2203 (1973).
[84]D. J. Tannor, *Introduction to Quantum Mechanics: A Time-Dependent Perspective* (University Science books: Mill Valley, U.S.A, 2007).
[85]J. H. Shirley, Phys. Rev. **138**, B979 (1965).
[86]A. Csehi, M. Kowalewski, G. J. Halász, and Á. Vibók, New J. Phys. **21**, 093040 (2019).
[87]L. Qiu, A. Mandal, O. Morshed, M. T. Meidenbauer, W. Girten, P. Huo, A. N. Vamivakas, and T. D. Krauss, J. Phys. Chem. Lett. **12**, 5030 (2021).
[88]T. E. Li, B. Cui, J. E. Subotnik, and A. Nitzan, Annu. Rev. Phys. Chem. **73** (2021), 10.1146/annurev-physchem-090519-042621.
[89]T. Schwartz, J. A. Hutchison, J. Léonard, C. Genet, S. Haacke, and T. W. Ebbesen, ChemPhysChem **14**, 125 (2013), https://chemistry-europe.onlinelibrary.wiley.com/doi/pdf/10.1002/cphc.201200734.
[90]A. Thomas, E. Devaux, K. Nagarajan, G. Rogez, M. Seidel, F. Richard, C. Genet, M. Drillon, and T. W. Ebbesen, Nano Lett. **21**, 4365 (2021).
[91]K. Nagarajan, A. Thomas, and T. W. Ebbesen, J. Am. Chem. Soc. **143**, 16877 (2021).
[92]K. Hirai, H. Ishikawa, T. Chervy, J. A. Hutchison, and H. Uji-i, Chem. Sci. **12**, 11986 (2021).
[93]K. Hirai and H. Uji-i, Chem. Lett. **50**, 727 (2021).
[94]S. Satapathy, M. Khatoniar, D. K. Parappuram, B. Liu, G. John, J. Feist, F. J. Garcia-Vidal, and V. M. Menon, Sci. Adv. **7**, eabj0997 (2021).
[95]W. M. Takele, F. Wackenhut, Q. Liu, L. Piatkowski, J. Waluk, and A. J. Meixner, J. Phys. Chem. C **125**, 14932 (2021).
[96]G. D. Wiesehan and W. Xiong, J. Chem. Phys. **155**, 241103 (2021).
[97]M. V. Imperatore, J. B. Asbury, and N. C. Giebink, J. Chem. Phys. **154**, 191103 (2021).
[98]J. Lather, A. N. K. Thabassum, J. Singh, and J. George, Chem. Sci. **13**, 195 (2022).
[99]R. H. Tichauer, J. Feist, and G. Groenhof, J. Chem. Phys. **154**, 104112 (2021).
[100]D. Sanvitto and S. Kéna-Cohen, Nat. Mater. **15**, 1061 (2016).
[101]K. Georgiou, K. E. McGhee, R. Jayaprakash, and D. G. Lidzey, J. Chem. Phys. **154**, 124309 (2021).
[102]D. Xu, A. Mandal, J. M. Baxter, S.-W. Cheng, I. Lee, H. Su, S. Liu, D. R. Reichman, and M. Delor, arXiv (2022), 10.48550/ARXIV.2205.01176, arxiv:2205.01176.
[103]K. Georgiou, R. Jayaprakash, A. Othonos, and D. G. Lidzey, Angew. Chem. Int. Ed. **60**, 16661 (2021).
[104]M. Balasubrahmaniyam, C. Genet, and T. Schwartz, Phys. Rev. B **103**, l241407 (2021).
[105]A. Graf, L. C. Tropf, Y. Zakharko, J. Zaumseil, and M. C. Gather, Nat. Commun. (2016), 10.17630/2baaf9f7-9e91-456a-ae0c-22f752d7f7b6.
[106]I. Vurgaftman, B. S. Simpkins, A. D. Dunkelberger, and J. C. Owrutsky, J. Phys. Chem. Lett. **11**, 3557 (2020).
[107]B. Xiang, R. F. Ribeiro, A. D. Dunkelberger, J. Wang, Y. Li, B. S. Simpkins, J. C. Owrutsky, J. Yuen-Zhou, and W. Xiong, Proc. Natl. Acad. Sci. **115**, 4845 (2018).
[108]Michalsky, Tom, Franke, Helena, Buschlinger, Robert, Peschel, Ulf, Grundmann, Marius, and Schmidt-Grund, Rüdiger, Eur. Phys. J. Appl. Phys. **74**, 30502 (2016).
[109]F. Hu and Z. Fei, Adv. Opt. Mater. **8**, 1901003 (2020), https://onlinelibrary.wiley.com/doi/pdf/10.1002/adom.201901003.
[110]A. M. Berghuis, V. Serpenti, M. Ramezani, S. Wang, and J. G. Rivas, J. Phys. Chem. C **124**, 12030 (2020).
[111]A. M. Berghuis, R. H. Tichauer, L. M. A. de Jong, I. Sokolovskii, P. Bai, M. Ramezani, S. Murai, G. Groenhof, and J. G. Rivas, ACS Photonics **9**, 2263 (2022).
[112]J. Guan, J.-E. Park, S. Deng, M. J. H. Tan, J. Hu, and T. W. Odom, Chem. Rev. **122**, 15177 (2022).
[113]R. Guo, T. K. Hakala, and P. Törmä, Phys. Rev. B **95**, 155423 (2017).
[114]S. Baieva, O. Hakamaa, G. Groenhof, T. T. Heikkilä, and J. J. Toppari, ACS Photonics **4**, 28 (2017).
[115]C. Brimont, L. Doyennette, G. Kreyder, F. Réveret, P. Disseix, F. Médard, J. Leymarie, E. Cambril, S. Bouchoule, M. Gromovyi, B. Alloing, S. Rennesson, F. Semond, J. Zúñiga-Pérez, and T. Guillet, Phys. Rev. Appl. **14**, 054060 (2020).
[116]J. J. Hopfield, Phys. Rev. **112**, 1555 (1958).
[117]J. Keeling, *Light-Matter Interactions and Quantum Optics* (University of St. Andrews, 2012).
[118]J. Li, D. Golez, G. Mazza, A. J. Millis, A. Georges, and M. Eckstein, Phys. Rev. B **101**, 205140 (2020).
[119]M. Amin, E. R. Koessler, O. Morshed, F. Awan, N. M. Cogan, R. Collison, T. Tumiel, W. Girten, C. S. Leiter, A. N. Vamivakas, P. Huo, and T. D. Krauss, ChemRxiv (2024), 10.26434/chemrxiv-2023-4tshv-v2.
[120]F. Freire-Fernández, N. G. Sinai, M. J. Hui Tan, S.-M. Park, E. R. Koessler, T. Krauss, P. Huo, and T. W. Odom, ACS Nano **18**, 15177 (2024), pMID: 38808728, https://doi.org/10.1021/acsnano.4c03164.
[121]R. S. Mulliken, J. Am. Chem. Soc. **74**, 811 (1952).
[122]N. S. Hush, "Intervalence-transfer absorption. part 2. theoretical considerations and spectroscopic data," in *Progress in Inorganic Chemistry* (John Wiley & Sons, Ltd, 1967) pp. 391–444, https://onlinelibrary.wiley.com/doi/pdf/10.1002/9780470166093.ch7.
[123]T. J. Giese and D. M. York, J. Chem. Phys. **120**, 7939 (2004).
[124]T. V. Voorhis, T. Kowalczyk, B. Kaduk, L.-P. Wang, C.-L. Cheng, and Q. Wu, Annu. Rev. Phys. Chem. **61**, 149 (2010).
[125]J. E. Subotnik, S. Yeganeh, R. J. Cave, and M. A. Ratner, J. Chem. Phys. **129**, 244101 (2008), https://doi.org/10.1063/1.3042233.
[126]M. Kowalewski, K. Bennett, and S. Mukamel, J. Phys. Chem. Lett. **7**, 2050 (2016).
[127]A. Mandal and P. Huo, J. Phys. Chem. Lett. **10**, 5519 (2019).
[128]J. Fregoni, G. Granucci, E. Coccia, M. Persico, and S. Corni, Nat. Commun. **9**, 4688 (2018).
[129]D. P. Craig and T. Thirunamachandran, *Molecular quantum electrodynamics: an introduction to radiation-molecule interactions* (Dover Publications, 1998) p. 324.
[130]G. Grynberg, A. Aspect, and C. Fabre, *Introduction to quantum optics from the semi-classical approach to quantized light* (Cambridge University Press, 2010) p. 665.